AUGUST 2019 M.Sc. in Civil Engineering OKBAH IBRAHIM KHALIL

REPUPLIC OF TURKEY

GAZİANTEP UNIVERSITY

GRADUATE SCHOOL OF NATURAL & APPLIED SCIENCES

INVESTIGATION OF FLEXURAL PERFORMANCE OF DOUBLE SKIN CONCRETE FILLED STEEL TUBE BEAMS

M.Sc.THESIS

IN

CIVIL ENGINEERING

BY

OKBAH IBRAHIM KHALIL

AUGUST 2019

INVESTIGATION OF FLEXURAL PERFORMANCE OF DOUBLE SKIN CONCRETE FILLED STEEL TUBE BEAMS

M.Sc. Thesis

in

Civil Engineering

Gaziantep University

Supervisor

Asst. Prof. Dr. Mehmet Tolga GÖĞÜŞ

by

Okbah Ibrahim KHALIL

August 2019

REPUBLIC OF TURKEY
GAZİANTEP UNIVERSITY
GRADUATE SCHOOL OF NATURAL & APPLIED SCIENCES
CIVIL ENGINEERING DEPARTMENT

Name of the Thesis : Investigation of Flexural Performance of Double Skin Concrete Filled Steel Tube Beams

Name of the Student : Okbah Ibrahim KHALIL

Exam Date : 20.08.2019

Approval of the Graduate School of Natural and Applied Sciences

Prof. Dr. A. Necmeddin YAZICI
Director

I certify that this thesis satisfies all the requirements as a thesis for the degree of Master of Science.

Prof. Dr. Hanifi ÇANAKCI
Head of Department

This is to certify that we have read this thesis and that in our consensus opinion it is fully adequate, in scope and quality, as a thesis for the degree of Master of Science.

Prof. Dr. Mehmet Tolga GÖĞÜŞ
Supervisor

Examining Committee Members:	Signature
Assoc. Prof. Dr.Amjad KHABAZ	…………………..
Assoc. Prof. Dr. Talha EKMEKYAPAR	…………………..
Asst. Prof. Dr. Mehmet Tolga GÖĞÜŞ	…………………..

I hereby declare that all information in this document has obtained and presented in accordance with academic rules and ethical conduct. I also declare that, as required by these rules and conduct, I have fully cited and referenced all material and results that are not original to this work.

Okbah Ibrahim KHALIL

ABSTRACT

INVESTIGATION OF FLEXURAL PERFORMANCE OF DOUBLE SKIN CONCRETE FILLED STEEL TUBE BEAMS

KHALIL, Okbah Ibrahim
M.Sc. in Civil Engineering
Supervisor: Asst. Prof. Dr. Mehmet Tolga GÖĞÜŞ
August 2019
54pages

Concrete Double Skin Steel Tube (CFDSST) beams are consist of two skins of steel filled with concrete between them. CFDSST member is lighter than Concrete Filled Steel Tube (CFST) members, which has a solid cross-section. Therefore, by lessening seismic force against the structures during an earthquake, the CFDST members can be effectively applied to the seismic resistance structures such as the high-rise buildings, bridge piers, etc. This thesis deals with are an experimental investigation of the effect of cross-section and the position of the inner tube on the flexural performance of CFDST beams. A total 13 CFDST beams specimens filled with self-compacted concrete was tested. The parameters examined in the test: (a) inner tube cross-section (square and rectangular) (b) the position of inner tube (center and bottom). Comparisons are presented between the examined specimens according to the flexural strength, failure modes, ductility and flexural stiffness.

Keywords: Concrete-Filled Double Skin Steel Tube (CFDSST) beams, Self-compacting concrete, Double skin, Flexural strength, Ductility.

ÇİFT CİDARLI BETON DOLDURULMUŞ ÇELİK TÜP KİRİŞLERİN EĞİLME PERFORMANSININ İNCELENMESİ

KHALIL, Okbah Ibrahim
Yüksek Lisans Tezi, İnşaat Mühendisliği
Danışman: Dr. Öğr. Üyesi Mehmet Tolga GÖĞÜŞ
Ağustos 2019
54 sayfa

Beton Doldurulmuş Çift Cidarlı Çelik Boru (BDÇCÇB) kirişler aralarında betonla doldurulmuş iki çelik cidardan oluşur. BDÇCÇB elemanlar, dolu kesiti olan beton doldurulmuş çelik tüp elemanlardan daha hafiftir. Bu nedenle, deprem sırasında yapılara karşı deprem kuvvet azaltılarak, BDÇCÇB elemanlar, yüksek katlı binalar, köprü iskeleleri vb. gibi depreme dayanıklı yapılara etkili bir şekilde uygulanabilir. Bu tez çalışması, iç tüpün kesit ve konumunun BDÇCÇB kirişlerinin eğilme performansı üzerine etkisi üzerine deneysel bir araştırmadır. Kendinden yerleşen betonla doldurulmuş toplam 13 BDÇCÇB kiriş örneği test edilmiştir. Testte incelenen parametreler: (a) iç boru kesit alanı (kare ve dikdörtgen) (b) iç boru pozisyonu (merkez ve alt). İncelenen numuneler arasında eğilme dayanımı, göçme modları, süneklik ve eğilme rijitliklerine göre bir karşılaştırmalar sunulmuştur.

Anahtar Kelimeler: Beton Doldurulmuş Çift Cidarlı Çelik Boru (BDÇCÇB) kirişler, Kendiliğinden yerleşen beton, Çift cidar, Eğilme dayanımı, Süneklik.

To my parents…...

ACKNOWLEDGEMENTS

I would like to express my special appreciation and thanks to my supervisor Asst. Prof. Dr. Mehmet Tolga GÖĞÜŞ, for all his help, patience, valuable advice, always providing and guiding me in the right direction. I am very grateful and proudest to work under his academic guidance.

Special thanks to my family. Words cannot express how grateful I am to my father that his words lead me to get certificates and my mother spirit for all of the sacrifices that have made on my behalf, and also to my brothers and sisters. I am grateful to my wife, for her strong encouragement and help me during my study.

TABLE OF CONTENTS

Page

LIST OF TABLES

Page

LIST OF FIGURES

LIST OF SYMBOLS

f_u	Ultimate strength of steel
f_y	Yield strength of steel
M_u	Moment capacity
D_u	Mid-span deflection at ultimate moment
DI	Ductility Index
k_i	Initial flexural strength
k_s	Serviceability flexural stiffness

LIST OF ABBREVIATIONS

f_u	Ultimate strength of steel
f_y	Yield strength of steel
M_u	Moment capacity
D_u	Mid-span deflection at ultimate moment
DI	Ductility Index
k_i	Initial flexural strength
k_s	Serviceability flexural stiffness
CFST	Concrete-Filled Steel Tube.
CFDSST	Concrete-Filled Double Skin Steel Tube.
SCC	Self-Compacted Concrete.
LVDT	Linear Variable Deferential Transistor

CHAPTER 1

INTRODUCTION

1.1 General

Concrete with steel are used in all construction work. There are several properties of steel, including the strength to tensile, compressive and high modulus of elasticity in addition to the ductility, resulting in long clear span structures and small size parts where big problem might be due to buckling as well as fire resistance. The resistance of the concrete to the tensile is weak but its resistance to compression is high in addition to the fire resistance and low cost, premature cracking and brittle crushing might be the most critical problems where resulting in massive bulk members. Concrete and steel can work together, compensate for each other and give high resistance to form composite structural part with predictable features.

(CFST) Tube progressively used as beam-column, beam and column in braced and un-braced frame structures (Mohanraj et al., 2010), (Elchalakani, M., et al., 2004) and (Ghannam, S. 2016). The composite construction structure provides numerous structural advantages contain high strength and resistance of fire, absorption capacity for high energy and favorable ductility, also during concrete construction the shutter use is not necessary. Therefore, costs of construction and time reduced. These features are widely used and have resulted in widespread use the tube filled with concrete in structures of civil engineering (Han et al., 2014). Also used all over the world is used as a primary lateral resistance from a compression member of an open-floor plan of a low-rise structure utilizing cold-formed steel tubes in-filled with in-situ concrete large caliber cast in situ or precast (Ghannam, S. 2016). The difficulty of compacting concrete is that concrete bleeding can create weaknesses in the system that creates gaps between steel and concrete. The Figure 1.1 and 1.2 show the applications CFST.

Figure 1.1 Wangcang East river bridge (Han and Bjorhovde, 2014).

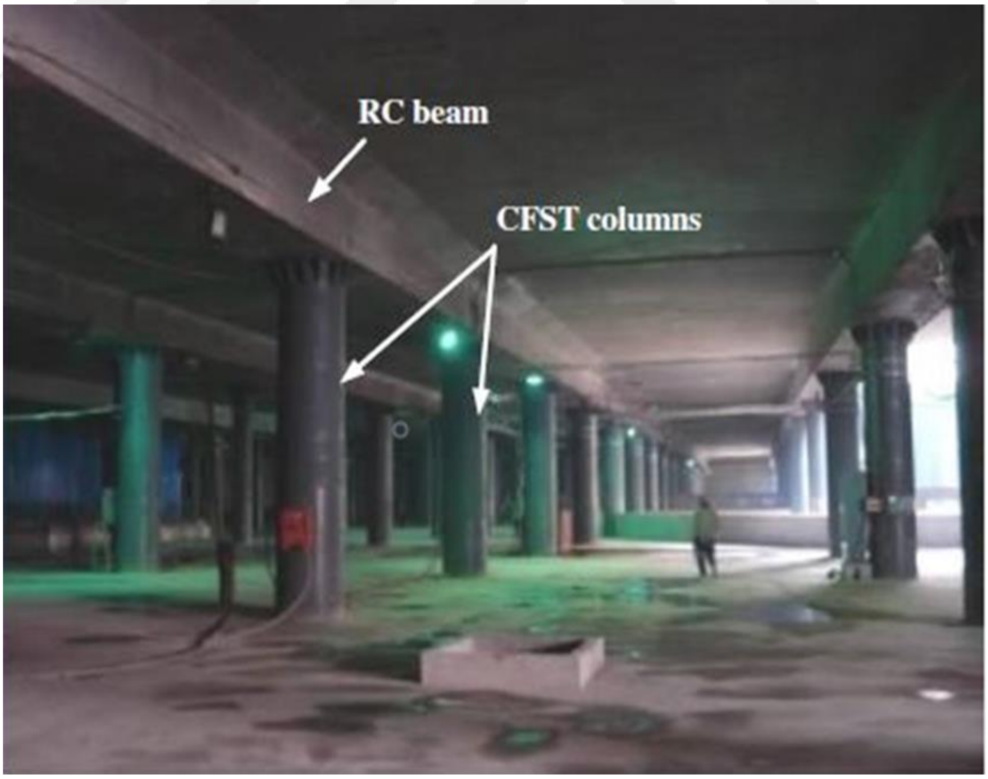

Figure 1.2 Subway station in Tianjin(Han and Bjorhovde, 2014).

CFDSST are composite structural members, can be recognized as a one kind of CFST, which consist of concrete that fills between the internal and external steel tube voids. The use of concrete filled steel tube has become famous in the last few decades. CFDSST help to reduce the self-weight and large energy absorption capacity against earthquake loading therefore have been used in high rise piers. Composite steel–concrete construction has recently been used in bridges and has been used in modern buildings and cities exposed to seismic hazards. The composite construction is ideally used in steel and concrete where the advantages are strength, hardness and light weight, low cost and quick completion of construction.

(Tao et al., 2004). Double reinforced steel tube is a creative invention for composite construction. Similar properties exist between CFDSST members and CFST members. In addition, they have high hardness Lighter weight, better cyclic performance, fill makes little contribution to the flexural stiffness due to the core area of a concrete while, and it increases the loading of the punch to the base of the column. Therefore, a new kind of composite member CFDSST with many features over CFST such as light weight, overall good Some researchers have suggested damping properties and improve cyclic performance. For CFDSST the internal tube give it many advantage such as light weight, high resistance for fire, high ductility, high stiffness and high moment capacity (Zhao and Han, 2006).

Self-compacting concrete (SCC) is used as filling the voids between external and internal steel tube beams in this study, it is well known that in a last years. SCC has significantly used in the concrete technology field, the introduction of SCC technology has greatly changed how to perform specific operations. It enables specific construction technology improvements to obtain results that are more efficient. By eliminating discontinuous mechanical vibrations, it is possible to improve the reliability of the concrete structure. The general strengthening of the working environment is cover by the improvement of health and safety of workers, which leads to improvement of productivity. The Figure 1.3 shows the application of CFDSST.

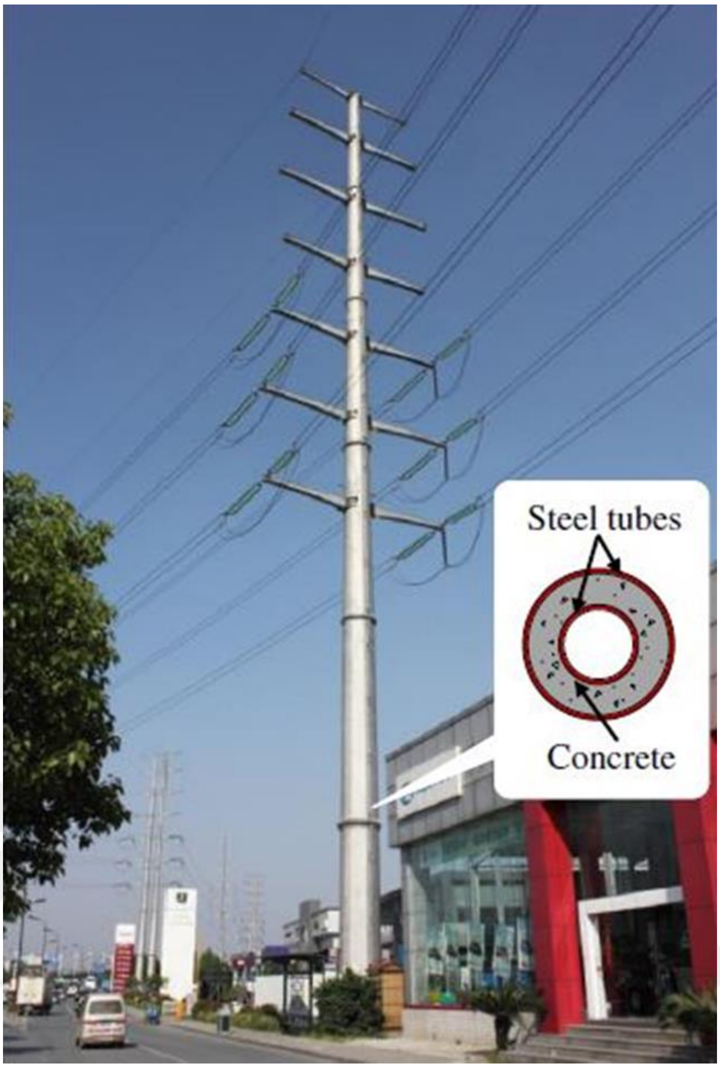

Figure 1.3 CFDSST pole (Han and Bjorhovde, 2014).

1.2 Objective of Study

In this study the main objective is investigate the flexural performance of double skin tube beam in terms of flexural strength (the stress in a material just before it yields in a flexure test), failure mode, ductility, flexural stiffness (is a standard for measuring deformability), weight and deflection through changing the shape of the inner tube where we use a square inner tube and use inner tube with equivalent area in rectangular shape and change the position of inner tube from the center to the bottom, the measurement of the outer tube is constant. Comparisons are made the effect of the different parameter on moment and ductility such as change the shape and position of inner tube.

Outline of the Thesis

Consists of five-chapter summary and abridgment of each chapter are given as below:

Chapter 1. Introduction:

A general and simplified explanation about CFST, CFDST.

Chapter 2. Literature review:

Previous research based on the scope of the study has been reviewed and maintained. A review of the literature and general background about CFST and CFDST.

Chapter 3. Experimental investigation:

This chapter provided an explanation and experimental investigation about the CFDST beam with applying for change shape, measurement and position of internal tube

Chapter 4. Results and discussion:

Results obtained from the double skin concrete filled tube beams experiment. Discussion of the results of the study was defined in this chapter.

Chapter 5. Conclusions:

Provide summary and conclusions depended on the results of comparative investigations of this study.

CHAPTER 2

LITERATURE REVIEW

2.1 Concrete Filled Steel Tube Members

CFST members take advantage of both concrete and steel. These consist of a circular or rectangular or section of steel hollow filled with reinforced or normal concrete. They are using widely as a beam of low-rise industrial buildings that require a rugged and efficient structural system and as high-rise buildings such as columns and beam-columns.

Han (2006) tested 36 samples of composite beam filled with SCC. In this study were four parameters varied in (1) cross section of beams (square and circular), (2) yielding strength of steel between 235 to 282 MPa, (3) the width of tube ratio to thickness of tube between 47 to 105, (4) the span of shear ratio to depth between 1.25 to 6. In this study found that the behavior of CFST beams filled with normal concrete are same to those filled with SCC. The capacity of moment for CFST beams could be calculated by using codes such as AIJ-1997, BS5400-1979, EC4-1994, AISC-LRFD-1999 and the model suggested by Han, It was noticed that EC4-1994 and Han’s model are a best predictors, the span of shear to depth ratio has no effect on the behaviors of the CFST sample with square and circular shapes. The simplified model for determining a moment-deformation diagrams of the samples has found. Comparisons between moment and curvature relationships presented, and mostly, good agreements were obtained.

Chapman (1964) studied a behaviour of 17 simply supported (CFST) under the concentration of distributed loads. The amount of shear connection was different within the range and the effect of interface slip-on elastic and ultimate load behavior was observed. It was observed that the use of ultimate load design for the composite steel-concrete section might lead to working stresses closed from the yield stress. Because of the large shape factor. This paper suggested that the connection of the shear should be designed to carry a horizontal shear force existing in the beam at ultimate load. For this objective, experimentally, 80% the inherent maximum capacity of the shear connector should be used. In the case of the uniformly loaded beam, uniform spacing of shear connectors proved to be satisfactory.

Adekola (1968) formulated the theory of interaction which picks account of slip, uplift and friction effects without assuming equal bends of interacting parts (mainly steel and concrete). The analysis of a differential element of the beam has led to two coupled simultaneous differential equations connecting the axial force within each of the parts with the uplift tension arising from differential deflections for the two parts. These equations in this study were then solved by the finite difference approach.

Yam and Chapman (1972) studied the elastic plastic behavior of composite beam of two spans experimental result. Concrete has no tensile strength; horizontal forces are transmitted through the reinforcement moment area. The computer program was written to solve the nonlinearity compute the differential equations using the predictor-corrector method. They are, the second hinge is formed in front of the first hinge, and therefore, a simple method of plastic design can be used. When a sufficient number of shearing connectors were separated uniformly between the points of maximum moment and minimum moment, Connectors will not occur. For continuous composite beams, slip may have a more significant effect with limited strain compatibility.

Han (2004) studied the behavior of concrete-filled hollow structure sections. A rectangular and square tube beams filled with normal concrete was tested. The parameter changed in the test was a ratio of the depth of the tube to the thickness of the wall between 20 to 50, the ratio of depth to width between 1 to 2. Due to the concrete voids, the concrete-filled steel rectangular hollow section and square hollow section beam tested worked relatively ductile way. The composite behavior of the concrete core and the steel tube improved the structural behavior of the column. The flexural strength of beams can be predicted by using the codes such as AIJ (1997), BS 5400 (1979), EC 4 (1994), LRFD-AISC (1999) Overall, AIJ (1997) and LRFD - AISC (1999) gave flexural strength about 20% lower than the test and BS 5400 (1979) about 12% lower than the experimental results. The method of AIJ (1997) is good for calculation of flexural rigidity of concrete-filled steel rectangular hollow section and square hollow section beams, also slightly lower stiffness value of intial flexural stifness and a slightly higher value of serviceability flexural stifness than the test results was predicted.

Assi and Hunaiti (2002) examined the partially wrapped composite beam theoretically and experimentally. In this study a 12 beams with length of 2.0 m and four different sizes are tested. The samples tested at two-point load. The eight beam specimens partially wrapped in normal concrete and lightweight concrete, three were hollow steel sections. To study the filling of different kinds of concrete against the capacity of ultimate moment for the partially wrapped section, four beams of three groups tested. The beam tested can reach a moment exceeding the theoretical prediction and therefore lightweight concrete can be consider a reliable part used for the composite structure also foamed concrete and lightweight aggregate filled steel beams were investigated. Thirty-four beam samples with square and rectangular shape and different depth to thickness ratios used in this study. For comparison purposes the samples filled with normal concrete and hollow steel were tested. In this study found that beams filled with lightweight aggregate and foamed concrete behaved flexural and were able to improving the strength of full flexural of their tubes. The load-deflection diagram found through the test with beams filled with light weight concrete. The bare steel section shown same behavior except an increase in ductility.

Zhou et al. (2017) studied a mechanical behavior of the CFSTs under axial tension. In this study were tested three group of circular CFSTs with different ratios of steel and in-filled concrete diameters and the results from study was compared with hollow steel tube . Relied on the results produced from experimental in the previous and present studies, three key issues of circular sample under tension, i.e., the confining stiffening influence, the tension-stiffening influence, and the confining-strengthening influence were studied at both levels of stress (i.e., stress-strain relation) and the level stress-resultant (i.e., force displacement relation). At the level of stress-resultant, the results of test explained that the circular stiffness and strength CFST were average 10% and 29% larger than those of hollow steel tube were, respectively. The result of reinforcement led to the increase in strength and there was a clear improvement in hardness, which is a result of joint hardening of granules and the effects of stress reinforcement at the level of stress through the experiment showed that the measured strains of circular tubes because of the difference of Poisson’s ratio between steel tube and filled concrete will be in the case of the double-axial tensile position will contribute to the reinforcement of the circular-shaped CFST.

Lai (2014) presented the evaluation and development of these design provisions. The CFST members have been reviewed available experimental databases and a modern experimental database for tests performed on non-compact and slender CFST has been compiled. For non-compact and slender CFST detailed 3dimension computer program finite element method have been sophisticated also used results of experimental to benchmark computer program finite element method. Design provisions of the AISC 360-10 for non-compact and slender CFST members have been evaluated by experimental test results and additional finite element method analysis dealing with experimental database gaps. The current AISC 360-10 axial load bending moment (P-M) interaction equation has been updated using the results of a comprehensive parametric study. Effective curves of stress-strain for steel tubes and concrete filled have also been advanced. Validating of these effective curves of stress-strain has been affirmed by implementing them in a macro model based on benchmarked nonlinear fiber analysis.

Alfawakhiri (1997) presented additional experimental data on the behavior of these structural elements and assess recent design code provisions with regard to circular CFST columns. Three long beam-columns that have length to diameter ratio of 13.5 were tested under continuous axial compression and incrementally enhanced reversals of lateral displacement. In addition, one short column was tested in concentric compression. All specimens had the same cross-sectional geometry to allow for direct comparison. Both strength and deformability issues were addressed. Various aspects of concrete confinement in circular CFST were analyzed. A comparative study of North American and European design code provisions was carried out. The result of the test indicates that by using of high strength concrete for circular CFST members does not cause any dramatic changes in the behavior. North American codes were shown to be more conservative than EC 4-1994, but all codes gave conservative predictions of strength compared to the experimental results. A less conservative design approach was recommended for CAN/CSA-S16.1-94.

Elchalakani (2001) in this study investigated the bending behaviour of CFST with circular section experimentally. The diameter ratio to thickness was in the range of 12 to 110. Under pure plastic bending a comparison was made between the behaviour of hollow sections and circular CFST. It was noticed that for the specimens which their depth to thickness ratios less than 40, for large rotations a local buckling prevented by void filling, while for specimens with depth to thickness between 74 to 110 multiple ripples of plastic created in the inelastic range it found that the filling of the tube of steel promotes, ductility, absorption of energy and strength for thinner sections. It concluded that the existing design rules for capacity of moment for circular concrete filled steel tubes could be extend to a new range (88-100).was recommended for CAN/CSA-S16.1-94.

Chitawadagi et al. (2009) prepared a study on the strength deformation behavior of circular steel tubes in-filled with concrete of different grade under bending. The influence of steel tube thickness, concrete filling strength, concrete cross sectional area and concrete confinement on curvature and moment capacity CFST were investigated. A comparison made between the measured flexural strength and the value predicted by EC 4-1994 and Load and Resistance Coefficient Design AISC-1999. A total of 99 samples with all lengths of 1 m was tested with concrete filling with characteristic strengths of 20, 30 and 40 MPa and a depth to thickness ratio of 22.3 to 50.8. Based on the investigational results, an interaction model has been developed to foresee the curvature and moment of the CFST specimens. The results indicate that in the experimental investigation are used to all the hollow section resistance moments and the corresponding increase in curvature showed higher ductility than the hollow. The ductility and resistance moment of both the hollow and the CFST sample are increased by increasing the wall thickness of the tube of steel. For a given wall thickness of the CFST specimen, increasing the strength of the filled concrete will not help to significantly increase its capacity. The Strength Increase Factor proposed here assists to estimate a contribution of concrete to the moment capacitance of the CFST beams. Detention of infill contributes of concrete to higher performance while higher strength infill concrete has been utilized for higher wall thickness steel tube. Furthermore, EC 4-1994 foresees the capacity of moment for the test samples moderately in the range of 30% to 35%. Since the influence of concrete filling is not taken into consideration and AISC / LRFD is also the same, it is very conservative to predict the capacity of moment for the CFST section.

Li et al. (2015) presented both experimental and numerical investigations on CFST tension members subjected to eccentric loads. Experimental parameters include load eccentricity and cross section steel ratio. Failure modes showed that in-filled concrete workings efficiently on steel tube and outside of tube improves concrete crack pattern and also modeling was used to predict the same result. The failure mode of CFST tension member subjected to eccentric load is a combination of elongation and all-inclusive bending. Composite members subjected to all eccentric loads showed large deformability when the rotation of the final end exceeded 0.1 rad. The compressive area may happen in the composite section while the member receives an eccentric load. Due to the composite effect of concrete and steel, the strength of composite specimen was much greater than hollow steel tube. The linear tension-to-moment interaction relationship shows acceptable results for CFST members. The recent design equation gives a safe and conventional estimate of the tension and flexural strength of CFST tension members subjected to eccentric forces.

Roeder et al. (2010) studied the combination of axial force and bending load and decided the best model to predict stiffness and circular resistance CFST. 122 specimen databases have been gathered and assessed. The result shows that the plastic stress way is a simple but effective method to predict the resistance of a circular CFST component under combined load. These data indicate that the current specification provides an inexact prediction of flexural stiffness and a representation of new stiffness is suggested. The suggested model allows simple but exact prediction of resistance and stiffness, allowing engineers to routinely use CFST constituents in structural design.

Varma et al. (2002) studied the experimental behavior for square CFST columns witches made from high strength material. The influence of strength, steel tube width to ratio of thickness, yield stress and axial load level on stiffness, and high strength ductility CFST beam column have been studied. 163/4 scale CFST samples containing eight monotonic beam-column samples and eight cyclic beam-column samples have been tested. Experimental results indicate that cyclic loading has no important influence on the strength or stiffness of the CFST beam column. However, it caused a more rapid diminution in the peak of post moment resistance.

Hu et al. (2011) were studied the behavior of fiber reinforced polymer confined circular CFST experimentally. The main varied parameters were the hoop stiffness of the glass fiber reinforcement polymer wrap and the ratio of the diameter to thickness for steel tube. 12 specimens tested in this study. All the samples were prepared such that the height was 400 mm and the outer diameter was around 200 mm. Therefore, the change in the diameter to thickness ratio is due to the change in steel tube thickness in the range of 1 to 2. The thickness of the glass fiber reinforced polymer wrap was 0.17 mm. Increasing the number of wrapping layers increased the rigidity of the wrapping. The results analyzed and a simplified equation for calculating the confinement effect of glass fiber reinforced polymer wrapping on concrete to the steel plate proposed. It was noticed that the use of glass fiber reinforced polymer wrapping led to delay the local buckling for the tube of steel within the CFST element.

Hsuan-Teh Hu (2003) studied the nonlinear finite element model of CFST using ABAQUS software and compared it with experimental data obtained from previous work. In numerical analysis, CSFT grouped into sections of squares and squares reinforced with conformal and circular sections, depending on the section. The behavior of the CFST sample studied and discussed depended on the geometric properties for the sample and the effect of a concrete pressure. The two test programs have six circular CFSTs and six square CFST. The thickness of the sample varied from 2 to 7.5 mm. In the case of the finite element method, since symmetry exists to shorten the program time, only 1/8 of the CFST specimen modeled. Numerical analysis revealed that the tube of steel gave a good confinement influence to the strength of concrete for the circular specimen especially when the width to thickness ratio was little. Steel for square specimens does not gave a large confining effect to concrete voids, especially when the ratio of width to thickness was big. In addition, by using the strap, the confinement effect of reinforced square CFST specimens improves, especially when the tie spacing is small and the tie number (or tie diameter) is large. In general this study focused on behavior of construction member and the tie number when the tie number increase the moment capacity increase. The results have confirm by using ABAQUS software.

2.2 Concrete Filled Double Skin Steel Tubes

Experimental studies conducted by You-Fu Yang (2015) on the performance of CFDSST beams. This studies exposed to local bearing forces. 16 samples were prepared and tested at an angle between the compressive member and bearing member 90º and 45º, whilst the sections of external and internal steel tubes of CFDSST samples were square hollow shapes. In the tests a major parameters were the external width ratio between compressive member and bearing member: from 0.4 to 0.6, the CFDSST hollow ratio: 0 to 0.6, the thickness of wall for external steel tube: 3.05 and 3.95 mm and bearing forces cross section: hollow and solid. The type of failure, load versus, bearing capacity deformation curve and corresponding deformation at the bearing capacity of the tested samples were analyzed and presented. Results of experiment showed that while exposed to local bearing forces. The samples of CFDSST have good resistance to deformation and high capacity of bearing. By using the proposed formulae were calculated the CFDSST capacities under local bearing forces in this study were evaluated by comparison with the result of experiment.

Hou (2015) behavior of circular CFDSST under local bearing forces was presented in his work. His study for CFDSST was an extension of previous research and studies on CFST. A many of tests were carried out, with some of the main parameters, including the load angle, hollow ratio, and the thickness of chord wall, also brace to chord diameter ratio. A test data was created and verified by computer program. An analysis of comparative for the full range behavior of CFST and CFDSST was performed under local bearing. CFDSST performance was found to be significantly affected by the internal tube, external tube and the sandwiched concrete, whilst it is capacity of bearing depended on the ratio of hollow. At last, relied on the analysis of load-transfer mechanism, simplified formulae for predicting the CFDSST strength under local bearing forces were presented. Sensible agreement was carried out between the measured values and predicted.

Uenaka and Hiroaki (2011) in their study they studied a common work of bending and shear through a three points static loading of CFDSST deep beam to look into mechanical behavior for the CFDSST. Two parameters of testing were looked, namely, the ratio of internal diameter to external diameter and the ratio of external tube diameter to thickness of external tube. Outcome showed the ratio of internal tube diameter to external tube diameter controlled on mode of failure. Their strengths for ratios of little than 0.47 agreed with the amount of estimation suggested herein. Moreover discussed a biaxial elastic plastic stress histories for both tubes beneath plane stress situation.

Han (2014) studied the behavior of tensile for CFDSST. In this study of an experimental on the eccentrically and concentrically loaded CFDSST tensile members was presented. The hollow ratio, the load eccentricity, and the nominal steel ratio of the cross section were included in the parameters of test. It was found that the double steel tubes efficiently with the filled concrete works, also found the tubes of steel under tension take additional support from filled concrete works. All eccentrically loaded of CFDSST tensile members with end rotation exceeding 0.1 rad exhibited a ductile behavior. Calculations of design were assessed. In this study was improved the proposal of existent design for CFDSST tensile member which was indicated by the results.

About CFDSST a series of tests was studied by Tao (2004). The specimen contained beam-columns (12) and (CFDST) stub columns (14) were performed. The external tube was circle and the internal tubes was square. The diameter-to-thickness ratio and hollow section ratio were the main parameters of experiment for stub columns while those for beam-columns were slenderness ratio and load eccentricity. In this research a theoretical model was sophisticated for CFDST beam-columns and stub columns. Where a confinement factor was inserted to depict the sample action between the sandwiched concrete and the external steel tube, a unified theory was described. The deformation relationships versus predicted load were in perfect agreement with beam-column and stub column results of test, a simplified models are derived to predict the load-carrying capacities of the composite members.

Uenaka (2013) made a asymmetric static four-point loading to research shear characteristics of deep CFDSST beams by experiment .He selected two main parameters, namely, the internal-to-external diameter ratios and the diameter-to-thickness. in this study found the shear resistance of CFDSST was decreased gradually as internal-to-external diameter ratio increased. Also provided mode to predict the shear resistance of deep CFDSST beams. In addition, discussed stress histories of both tubes through based upon their elastic-plastic stress behavior beneath plane stress situation.

Wang et al (2016) studied the behavior of thin-walled dodecagonal section CFDSST beneath bending. Both finite element analysis and experimental investigation were achieved. In this research tested seven samples that length each of these beam 2000 mm. The ratio of width to thickness for the external steel tube ranged from 75 to 133. From a test samples the results obtained the failure mode load- displacement curves and ultimate capacity. In this study developed finite element model. The results of test were verified against the finite element method results and by utilizing the verified model a parametric investigation was directed. Also, suggested manner was evaluated for thin-walled circular sample CFDSST subjected to bending.

On CFDSST beams, stub columns and beam–columns series of tests performed by Han et al (2006) the external and internal tubes were cold-formed rectangular hollow sections. Those of empty double skin tubular members and conventional concrete-filled steel tubular members were compared with the load–deformation behaviour and failure modes of CFDSST samples. A theoretical model in this studying was developed for the CFDSST beams, stub columns, and beam–columns. Reasonably perfect agreement was noticed between the tested curves and predicted. Simplified models were derived to predict the capacities of load-carrying for the composite members

Zhao and Grzebieta (1999) experimental investigation was conducted for a void-filled square hollow section beams subjected to large deformation period bending. The samples used for the test were of different depth to thickness ratios. The filler was of conventional concrete, lightweight concrete and polyurethane. The rig of cyclic test was developed. As each samples bent to a maximum of 20°, comparison made between the previous test result of the empty square hollow section beam and the result of this study test. The results showed that for all packing materials tested the increase in rotation angle at the final moment was 300%. The increasing in the capacity of ultimate moment was mainly dependent on filling material strength. It also observed that lightweight filler material or lightweight concrete could be used for non-compact and compact sections to achieve an acceptable mechanism.

Hou et al (2015) presented research on the accurate behavior of CFDSST under the influence of local bearing. A chain of analyses was carried out depended on varied parameters, including hollow ratio, loading angle and chord wall thickness. This laboratory work can be considered as a complementary work of old laboratory works on the CFST units. A method of computer program has been employed and confirmed through applying testing data. In this study, some differentiations have been proceeded between the action of CFDSST and CFST through the effect of the local bearing. The resultant clarified that the performance of members that have double tubes were better than the member section comprised of one tube because of the effect of the interaction and collaboration between the outer skin, inner skin, and sandwiched concrete. It was also found that the capacity of bearing relied on the hollow ratio. The measured and prophesied values gave reasonable agreement.

Tao (2004) studied on CFDSST a series of tests were achieved the test it contain CFDSST beams (4), stub columns (14), and beam -columns (12). The samples had an external was square hollow section and internal skin shape was hollow circular section. Mechanical model for the CFDSST stub columns, columns and beam-columns was developed in this research uniform theory was described in which the factor of confinement was inserted to explain the composite action between sandwiched concrete and the tubes of steel. The relationship of axial strain versus load for CFDSST stub columns was predicted. Deriving the simplified form against the CFDSST section capacity. A comparison was made between the predicted beam-column strength and that obtained in beam and beam-column tests. The relationship of load versus mid-span deflection for CFDSST beams and beam-columns was predicted. Also the researcher was developed simplified model calculating the member capacity of the CFDSST beams. Simplified interaction curves are derived for CFDSST beam-columns.

Idris and Ozbakkaloglu (2015) investigated the experimental behavior using the new system of the CFDSST beam by replacing the external steel skin by the fiber reinforcement polymer. Four samples databases have been gathered and assessed for investigating its cyclic conduct. High-strength was the feature that characterizes the concrete used in this study. Three centered parameters were depended in this work namely, both of the two skins dimensions, the presence of the stuffed concrete and the fitting of the ring that fixed about the internal skin. After looking at the results, it became clear that the most prominent characteristic of this sort of beams is the great ductility resulting from presence of fiber reinforcement polymer material. The results also showed that the displacement resulted of side loading were small when the dimensions of internal tube were a large while, the displacement became large when the dimensions of internal tube became small. This condition was achieved only when the external tube was made of fiber reinforcement polymer material. It was observed that adding of constructional connectors on the internal skin and concrete-filling the tube both affect the overall behavior and side deflection of the fiber reinforcement polymer beam. Furthermore, the results highlighted that through the using of connectors the slip between the tubes surfaces and the concrete surface can be completely canceled.

Amanana et al. (2017) conducted a study on the mechanical properties of the CFDSST. The compressive for cubes and split tensile for cylinder were tested at 7, 14 and 28 days. 24 CFDSST beam tested and observed increased the flexural strength with respected to the increase in the measurement of internal tube by keeping the external tube measurement as constant and changing the internal steel tube measurement. Experimental results have been compared with predictive results.

Tao (2006) described a chain of performed tests on CFDSST, beams, stub columns and beam columns. Rectangular hollow section cold-formed both outside of the tube and inside of the tube. The fracture mode and behavior of load deformation for CFDSST samples have been compared with those of conventional CFST samples and empty double-skin tube members. The results observed that the CFDSST samples displayed behaviors similar to the conservative CFST samples in the present test. Improvement in ductility and strength were observed for CFDSST (rectangular hollow section external and internal), beams stub columns and beam columns due to the composite action between the concrete core and the steel tube. A theoretical model has been advanced to foresee the deformation versus load relationship of CFDSST beam stub column, and beam column. A pretty agreement has been attained between the prediction curve and the experimental curve. Simplified models were advanced to assess the strength of CFDSST beam-columns, beams and columns. With reasonable agreement achieved, all predictions were compared with the result of tests.

Wang (2018) in this study conducted Structural performance of CFDSST beams with eccentric internal tubes. The external tube made from stainless steel, the internal tube made from carbon steel. The sample was tested under three points. From the results test observed that the sample has the internal tube in the tensile position gave bending moment greater than the sample has internal tube in the center .The results were compared with the expected results based on the European and American specifications. The external tube was rectangular, the internal tube was circle. The Figure 2.1 shows the form of the specimen used in the experiment.

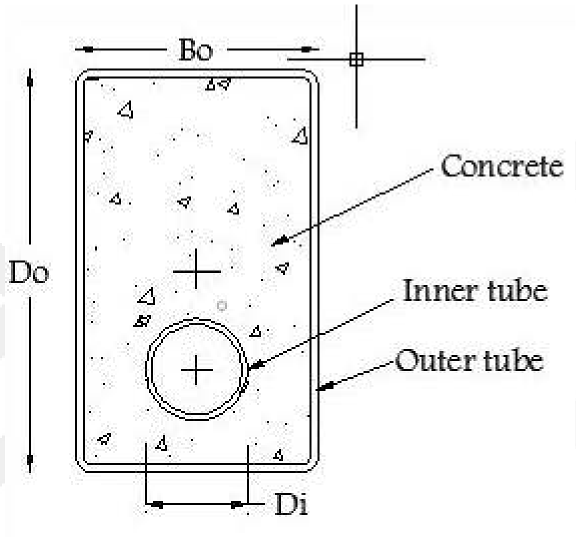

Figure 2.1 The form of the specimen used in the experiment.

Han et al. (2014) studied the CFDSST structure and draw out the research framework of CFDSST samples. Recent CFDSST structural members, especially research and development in China, have been summarized and discussed. In China some projects utilizing CFDSST members have also been introduced. At last, many conclusions were given for CFDSST members. The results observed that the internal tube provided influence support to the sandwich concrete, and the behavior of the composite sample was same to that of the concrete-filled steel tube, after beam and column ultimate strength tests the inward buckling of the internal tube and the outward buckling of the external tube was observed .The steel tubes and a concrete can work at the same time well and the integrity of the steel-concrete was maintained on the interface. fire resistance for the CFDSST column best than fire resistance for regular CFST columns due to the sandwiched concrete was protected internal tubes during fire, when designing members with large cross-sections the CFDSST could be a good option. Figure 2.2 showed a cross-section of a typical CFDSST.

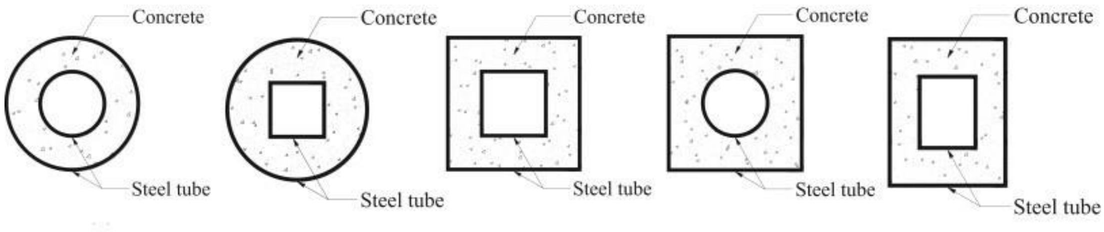

Figure 2.2 Concrete-filled double skin steel tubes (CFDSST)

CHAPTER 3

EXPERIMENTAL INVESTIGATION

3.1 General

The experimental investigation was accepted to study the flexural performance of double skin concrete filled tube beams. The study focused on the flexural bending behavior through a series of twelve CFDSST and one control steel tube beams. The parameters considered are the effect of the inner tube by changing the location of inner tube from center to bottom (tension zone) and changing the shape from a rectangle to square with maintaining the equal area between them. The CFDSST specimens was compared with control beam. This chapter presents properties and details of the materials are used to construct the specimens and testing of the specimens.

3.2 Material Properties

3.2.1 Self-Compacted Concrete

In this study, the mix ratio of the SCC consisted of Water (W), Super Plasticizer (SP), Cement (C), Fly Ash (FA), Natural sand(NS),Crushed Sand (CS) with range of particle sizes are 2-0.3mm, and <0.3mm as finer, and Course Aggregate (CA) are used. The mix design is done for M40 grade, the water-binder ratio (W/B) is used as 0.33, and the mix proportion of SCC is given in Table 3.1 below. The mean compressive strength of the mix proportion is determined in the laboratory at testing day after casting of three cylinders 100mm by 200 mm as shown in Figure 3.1. The average strength for concrete compressive is 48.6 MPa. The split tensile of concrete is obtained by applying compressive force along the length of concrete cylinder The mean split tensile strength of the mix proportion is determined in the laboratory at testing day after casting of three cylinders 100 mm by 200 mm as shown in Figure 3.2. The result of split tensile strength received from Equation 3.1. The average concrete tensile strength is 12.28 MPa.

$$T = 2P / \pi LD \tag{3.1}$$

Where:

T = splitting tensile strength, MPa

P = maximum applied load, N

D = diameter of the specimen, mm

L = length of the specimen, mm

Table 3.1 Mix proportions of SCC.

Mix proportion	W/B	C	FA	W	SP	CA	NS	CS 2-0.3 mm	CS 0.3 mm
Kg/m^3	2338.3	285	285	188.1	2.77	709.8	650.6	144.6	72.3

(a) (b)

Figure 3.1(a) Specimens before compressive test **(b)** Specimens after Compressive test

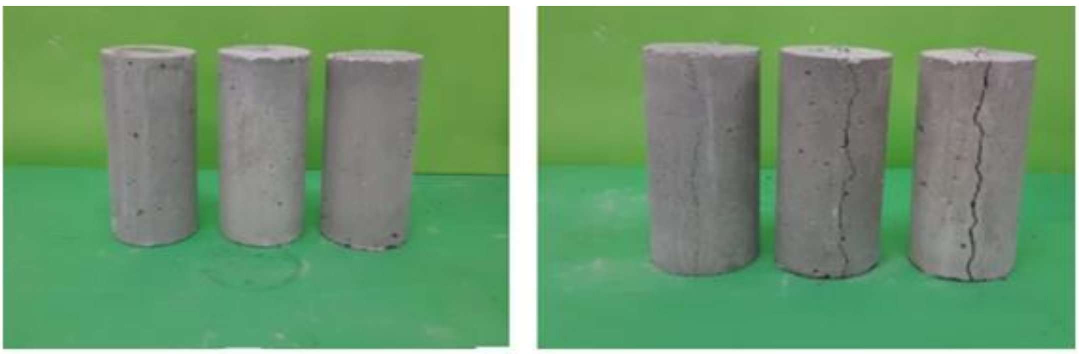

(a) (b)

Figure 3.2 **(a)** Specimens before split test **(b)** Specimens after split test.

3.2.2 Steel Tubes

In this study used 13 beam samples. All steel tubes are manufactured from cold hollow square and rectangular sections with a length of 6 meters. The nominal dimensions of the square steel tube sections were 810 x 100 x100 x 3 mm, 810 x 50 x 50x 2mm, 810 x 40 x40 x 2 mm and 810 x 30 x30 x 2 mm .The nominal dimensions of the rectangular steel tube sections were 810 x 60 x40 x 2 mm, 810 x 50 x30 x2 mm and 810 x 40 x 20 x 2 mm. The Figure 3.3 and 3.4 shows measurement and shape of the steel tubes.

Figure 3.3 The steel tubes specimens

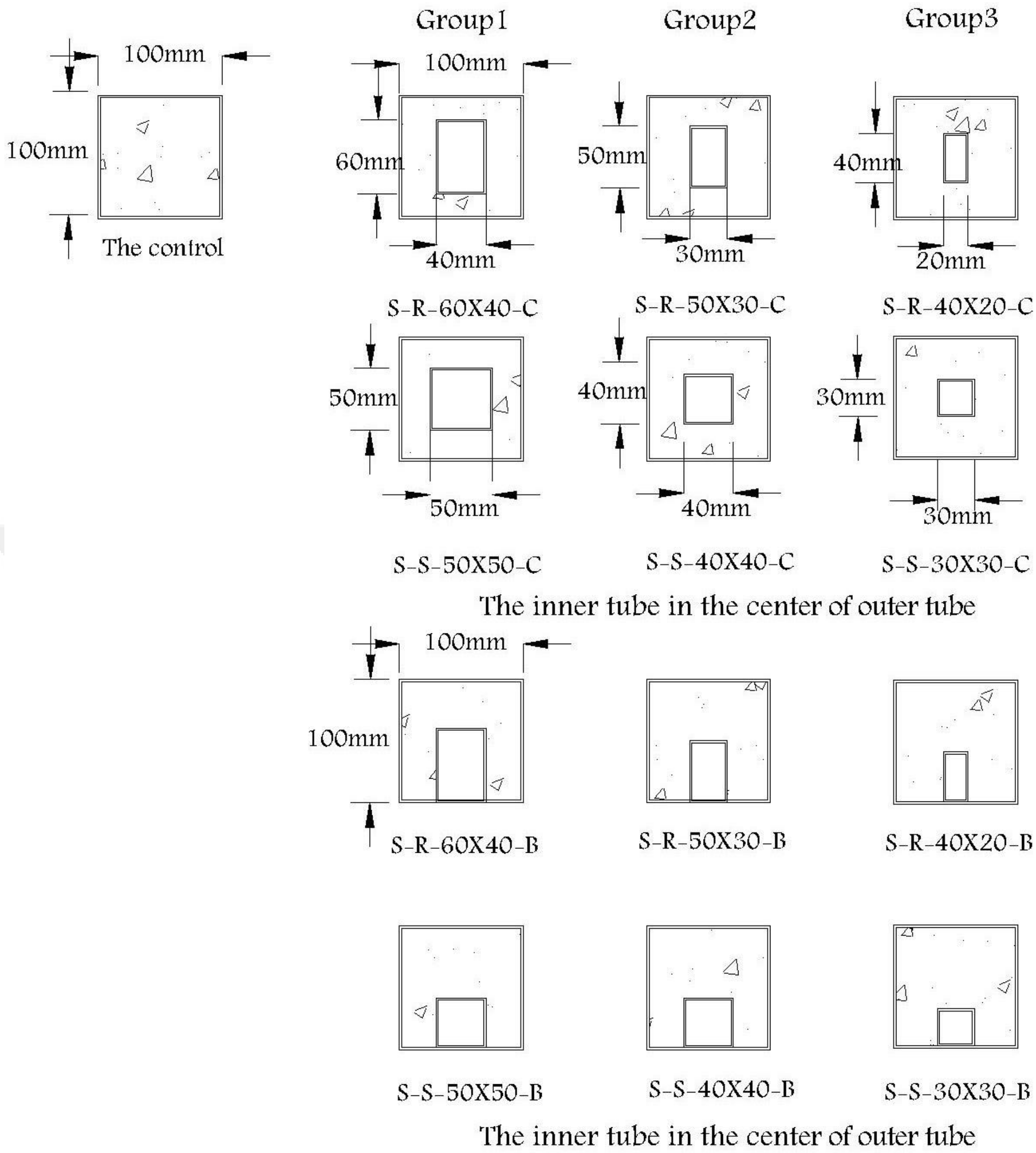

Figure 3.4 The dimensions of steel tubes

Three coupons for square tube and two coupons for rectangular tube were cut from sides of hollow steel sections to find the properties of the actual material. Tensile coupons were taken from all faces except for the welded face in the tubing to avoid uneven power due to welding. The tensile strength tests were performed and tested in accordance with the recommendations of ASTM E8 / E8M-15a (2015) (ASTM E8 / E8M-15a, 2015). Figure 3.4 (a) and (b) shows the coupon shape before and after test. Table 3.2 shows the properties of steel coupons.

Figure 3.5 (a) Tensile specimens before testing.

Figure 3.5 (b) Tensile specimens after testing.

Table 3.2 Properties of steel plates.

No.	measurement of tube(mm)	Thickness (mm)	Yield strength f_y (MPa)	Yield strength f_u (MPa)
1	100X100	3	265.24	467.1
2	60X40	2	256.5	483.21
3	50X50	2	365.36	377.96
4	50X30	2	323.33	365.90
5	40X40	2	293.73	390.11
6	40X20	2	333.34	418.93
7	30X30	2	270.36	375.79

3.3 Specimen Properties

Seven types of tubes were cut and formed with a thickness of 3 mm for outer tube and 2 mm for inner tube, square and rectangular steel in shape with a length of six meters and formed to the required length. The interior faces of the beam samples have been cleaned to remove any rust or debris, and the grease and oil deposits, if any, are cleaned. 13 samples were prepared from square and rectangular sections of length 810 mm for testing in this study. The 13 samples consist varied in the tests were; (1) the measurement of the inner tubes (2) the shape of the inner tubes square and rectangular (3) the position of inner tubes, groups of tubes are placed in the inner center of the outer tubes and the other groups placed in the bottom of the outer tube (tension zone) The samples were divided into three groups and one sample is control.

The following labeling system was used to assign each sample of the packages in Table 3.3 to illustrate the samples signs take the first Group for example , S-R-60X40-C refer to (S) outer tube is square(R) inner tube is rectangular (C) the position of inner tube in the center of outer tube , S-S-50X50-C refer to (S) outer tube is square(S) inner tube is square C the position of inner tube in the center of outer tube, S-R-60X40-B refer to (S) outer tube is square(R) inner tube is rectangular (B) the position of inner tube in the bottom edge of outer tube, S-S-50X50-B refer to (S) outer tube is square(S) inner tube is square B the position of inner tube in the bottom edge of outer tube.(t_o) represents the thickness of outer tube,(t_i) represents the thickness of inner tube.

The removable silicon later to prevent the leakage of the concrete mixture from which the steel tubes are held upright in the concrete-prepared rack closes the small spaces between the beam and bottom cover. The bottom ends of the steel tube are tightly covered with 2mm steel thickness by welding, then the SCC is poured into the steel tubes from the top without any compaction. After the filling, the concrete is cut using a shovel after the treatment period, in the event of any shrinkage, the gap is sealed using epoxy as show in Figure 3.6 and 3.7 and then covered with other steel plates by welding; a metal angle is installed on the model for carrying the linear variable differential transistors as shown in Figure 3.8.Samples were prepared for testing.

Figure 3.6 Specimens from cross section before casting.

Figure 3.7 Specimens after casting.

Figure 3.8 The specimens after install steel plate cover

Table 3.3 Dimension of steel tubes after cutting for all groups.

Group name	Tube designation	Length mm	Exterior dimension		Interior dimension		Positon of inner tube	t_o^* mm	t_i^{**} mm
			Height	Width	Height	Width			
1	S-R-60X40-C	810	100	100	60	40	Center	3	2
	S-S-50 X 50-C	810	100	100	50	50	Center	3	2
	S-R-60 X 40-B	810	100	100	60	40	Bottom	3	2
	S-S-50 X 50-B	810	100	100	50	50	Bottom	3	2
2	S-R-50 X 30-C	810	100	100	50	30	Center	3	2
	S-S-40 X 40-C	810	100	100	40	40	Center	3	2
	S-R-50 X 30-B	810	100	100	50	30	Bottom	3	2
	S-S-40 X 40-B	810	100	100	40	40	Bottom	3	2
3	S-R-40 X 20-C	810	100	100	40	20	Center	3	2
	S-S-30 X 30-C	810	100	100	30	30	Center	3	2
	S-R-40 X 20-B	810	100	100	40	20	Bottom	3	2
	S-S-30 X 30-B	810	100	100	30	30	Bottom	3	2
	Control	810	100	100	----	------	-------	3	-----

* Thickness of outer tubes

** Thickness of inner tubes

3.4 Test Procedure

The testing of beams is done by using of flexure machine test with 500 KN capacity. All beams are tested under simply supported end conditions and under two-point loading with displacement control loading method with a rate of 1mm / min. Since a support is fixed at a distance of 30 mm from both ends of the beam so the clear span is 750 mm. Two points loading is adopted for the test and it provides a net bending area of 250 mm. As shown in Figure 3.9 and 3.10

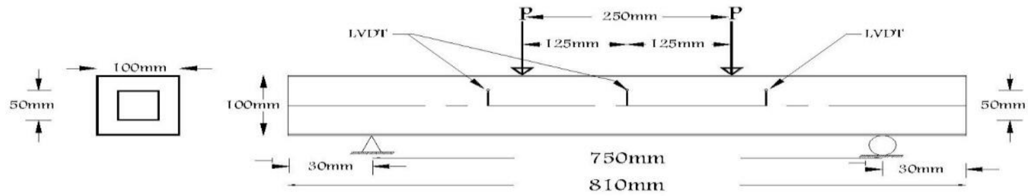

Figure 3.9 Effective dimension of flexural test on CFDSST

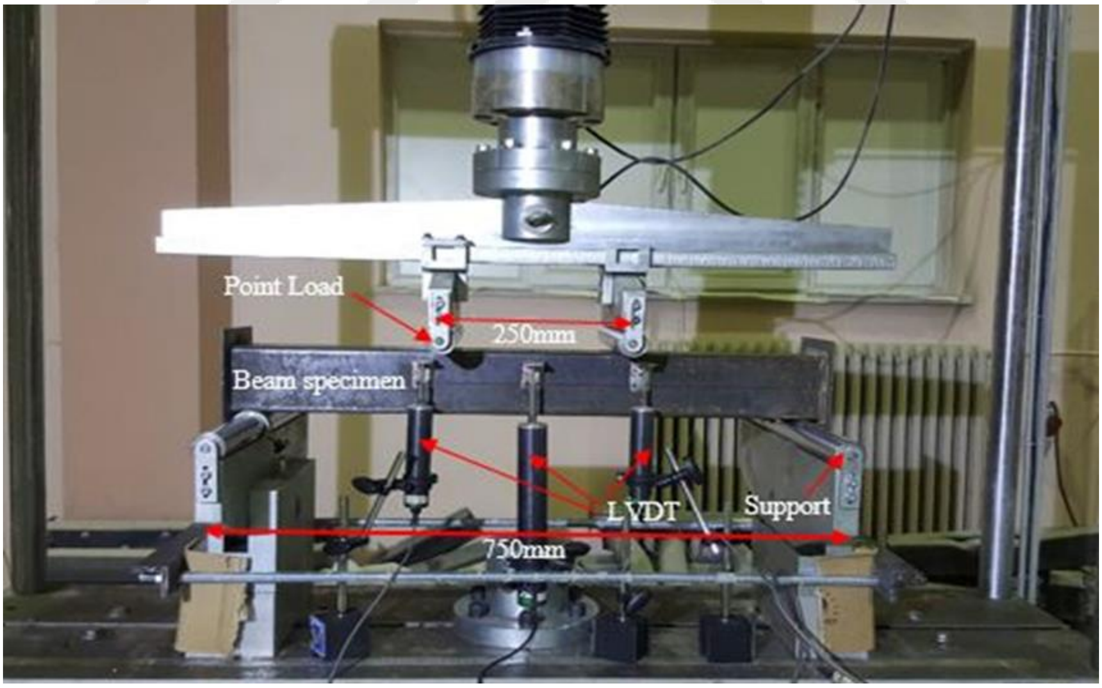

Figure 3.10 Flexure test on CFDSST beam.

The axis of the sample is carefully aligned with the axis of the loading device. Three linear variable differential transistors linear variable differential transistors are fixed along the length of the beam to measure the deflection. Among the three linear variable differential transistors, two are located at a distance of 150 mm on both sides from the mid span, the third linear variable differential transistors is fixed exactly at the mid-span. All beams are loaded up to failure. Pure bending is a condition of stress where a bending moment is applied to a beam without the simultaneous presence of axial, shear, or torsional force.

CHAPTER 4

RESULTS AND DISCUSSIONS

After the age of testing day, all beams are prepared for testing. The beams have been loaded with equal force on the two load points until it did not take any further load. First, the effect of control beam has been compared with all groups, it found that the inner tube inside the outer tube and concrete between them has significantly for increasing the beams moment carrying capacity and reduce the deflection; it means that the CFDST have a stiffer response for loading until failure occurred.

4.1 Failure Modes

The typical failure mode of the CFDSST beams was a local (outward buckling) for outer tube in the compression side of the tube near the points of load at ultimate moment capacity also rupture occurred at the end of test. According to the test results, the sample can be divided into many typical failure modes. For the group one the specimen one S-R-60X40-C happened outward local buckling for outer tube in the end of testing are occurred with rupture, the specimen two S-S-50X50-C happened two outward local buckling in the side and top for the outer tube also at the end of testing are occurred with rupture. Specimen three S-R-60X40-B happened outward local buckling for outer tube at the end of testing are occurred with rupture, in the corner of bottom edge while the specimen four S-S-50X50-B happened outward local buckling in two point for outer tube beam at the end of testing are occurred with rupture. The failure mode for Group one showed in Figure 4.1.

Figure 4.1 Failure modes for group one

For the group two the specimen one S-R-50X30-C happened outward local buckling for outer tube in the end of testing are occurred with rupture in bottom, the specimen two S-S-40X40-C happened outward local buckling in the outer tube at the end of testing are occurred with rupture in the corner of bottom edge also specimen three S-R-50X30-B and S-S-40X40-B happened outward local buckling at for outer tube at the end of testing are occurred with rupture, in the corner of bottom edge. The failure mode for group two showed in Figure 4.2.

Figure 4.2 Failure modes for group two

For the group three the specimen one S-R-40X20-C happened outward local buckling for outer tube at the end of testing are occurred with rupture in bottom, the specimen two S-S-30X30-C happened outward local buckling in the side and top for the outer tube at the end of testing are occurred with rupture in the corner of bottom edge. Specimen three S-R-40X20-B and Specimen four S-R-30X30-B outward local buckling happened for outer tube at the end of testing are occurred with rupture in the corner of bottom edge. The failure mode for Group three showed in Figure 4.3.

Figure 4.3 Failure modes for group three

For control beam outward local buckling happened in end of testing with rupture, the failure mode showed in Figure 4.4.

Figure 4.4 Failure modes for control

4.2 Deflection Curves along Effective Length

Maximum deflection occurs at the center point. In the case of two support points it will be at the midpoint between them regardless of the location of the point loads. Where there are more than two supports then it will be at a midpoint between the sections which has the most load. When loads are applied and increases gradually on the beam models, the member responses occur in the form of deformation. The initial beam conditions are attainable when the models undergo elastic deformation. The beam models followed approximately the half sine wave curve during the course of the total test. Also for CFDSST beams the X – axis represents the effective length and the Y – axis represents the deflection corresponding to different ultimate moment levels. It take control and group two from all groups and made a comparison between the specimens in this group, in this test observed the maximum deflection for the specimen S-S-40X40-B which equal 13.821 mm and the minimum deflection for the specimen S-S-40X40-C which was 12.307 mm that means the deflection is increase when change the position of inner tube for square shape from center to bottom also we observed the deflection for specimen S-R-50X30-C is larger than the deflection for specimen S-R-50X30-B which their value 13.195 and 12.411 respectively. The deflection for control greater than all specimen in group two. The deflection diagram is observed as show in Figure 4.5- 4.9.

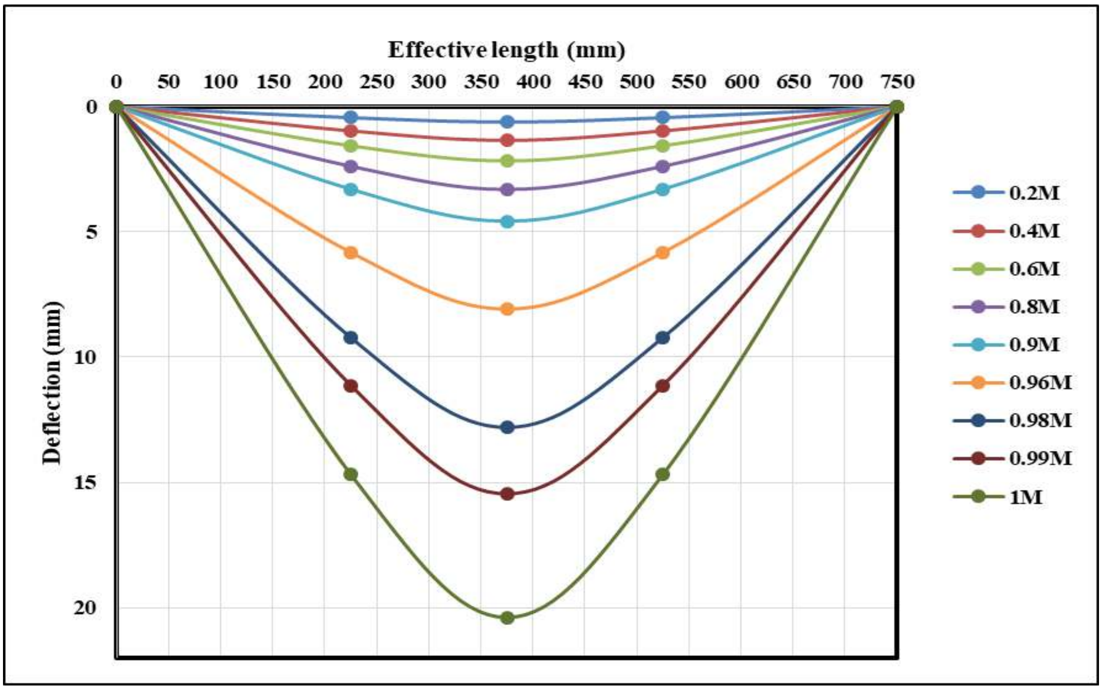

Figure 4.5 Deflection shape for control

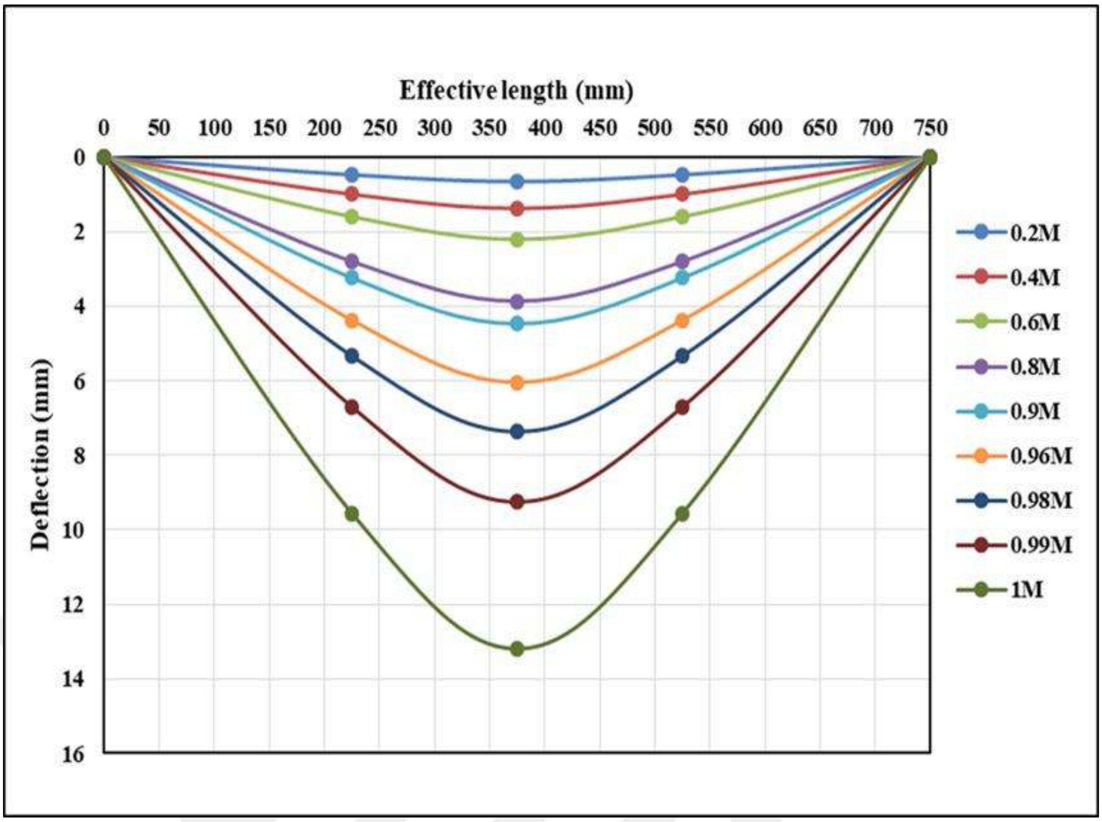

Figure 4.6 Deflection shape for specimen S-R-50X30-C in group two

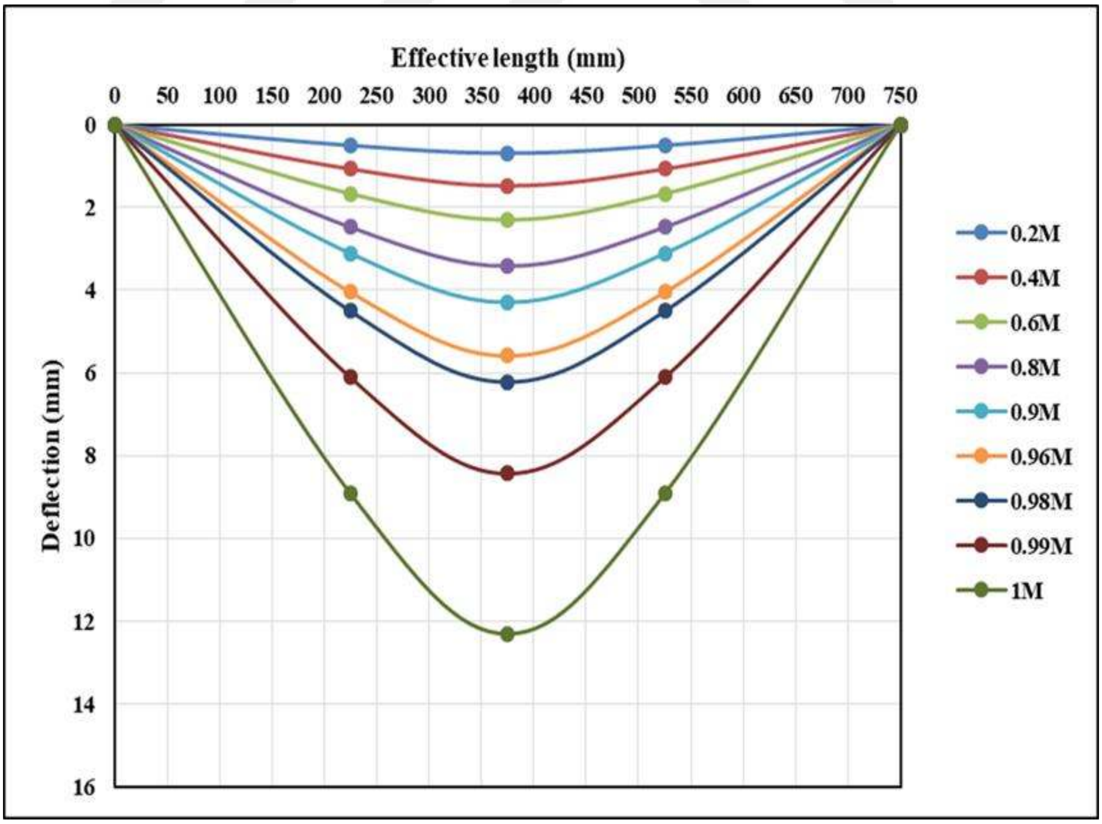

Figure 4.7 Deflection shape for specimen S-S-40X40-C in group two

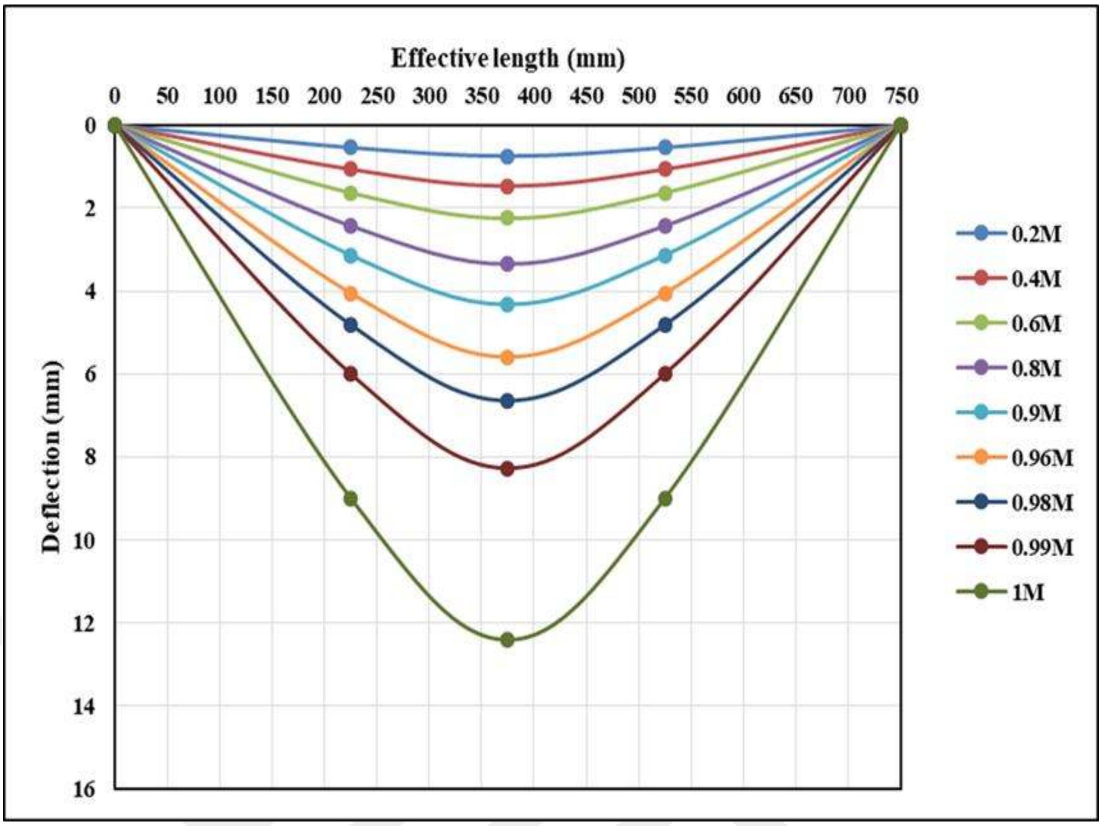

Figure 4.8 Deflection shape for specimen S-R-50X30-B in group two

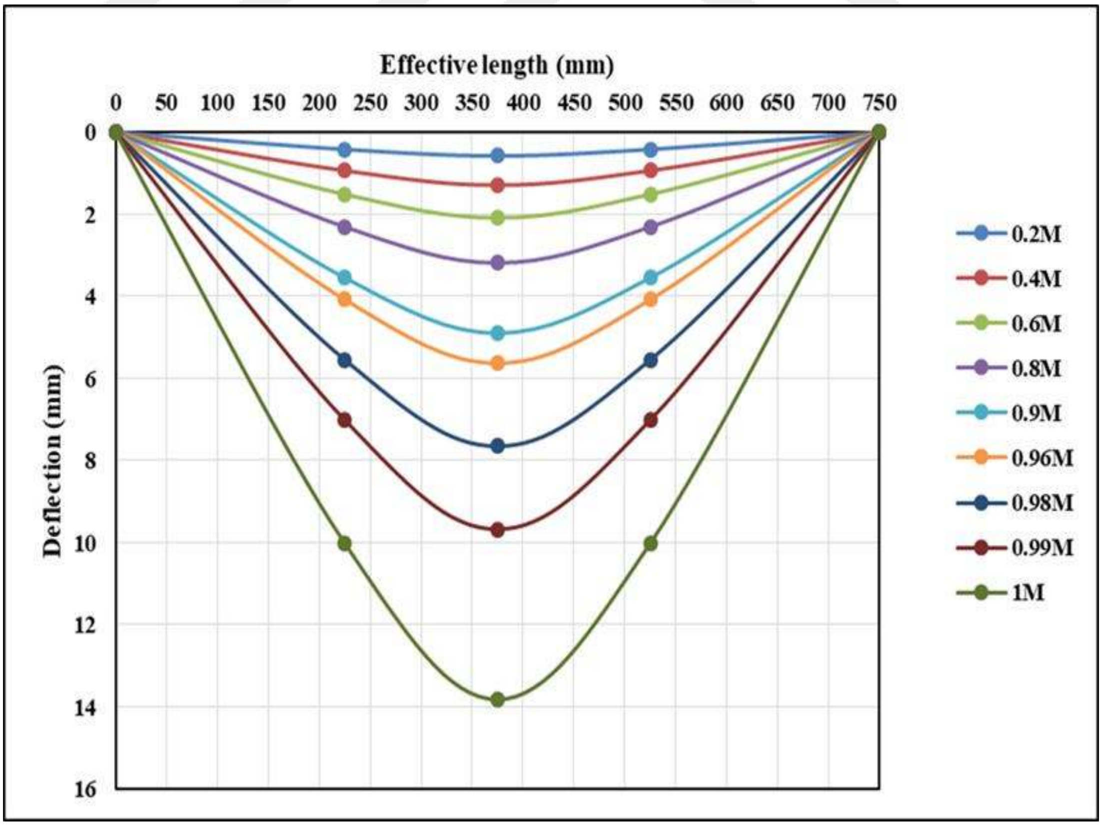

Figure 4.9 Deflection shape for specimen S-S-40X40-B in group two

In all CFDSST beams in this group, the effect of position of inner tube from center to bottom (tension zone) and use square shape the deflection is absolutely recognized. This feasibility indicates move the position of inner tube from center to bottom and use square shape increase the deflection.

4.3 Moment - Mid Span Deflection Relations

The moment – mid span deflection curves for all groups up to failure as shown in Figure 4.10. All the beams showed a smooth moment deflection curve with large deflection up to failure.

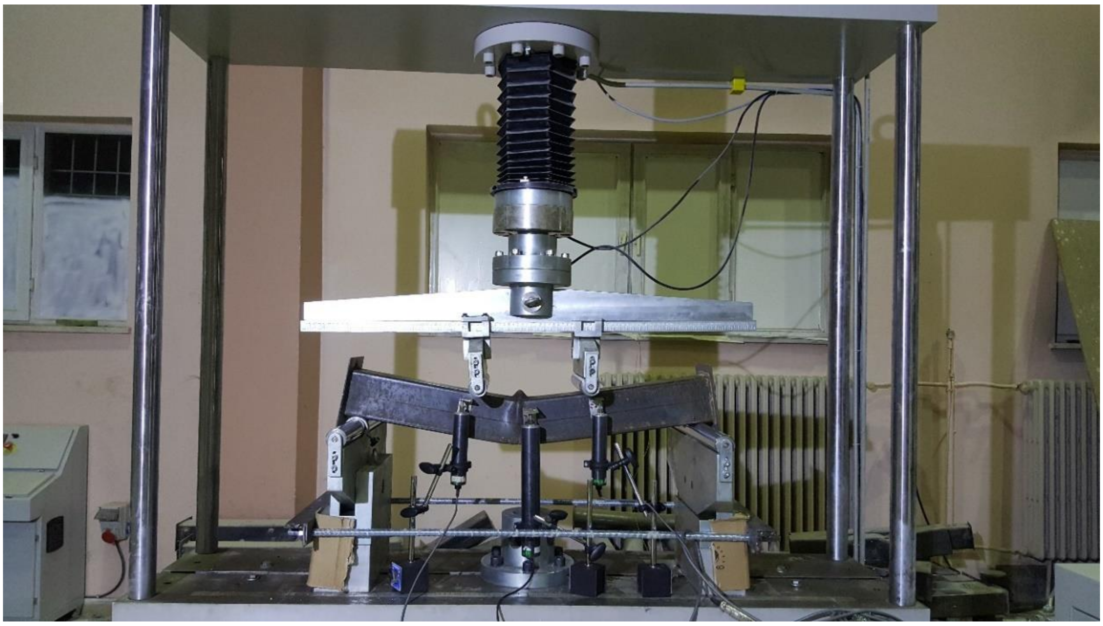

Figure 4.10 Failure pattern of CFDSST beam.

The CFST beam have been compared with all specimens CFDSST for all groups, it found that the inner tube with concrete inside the outer tubes have significantly increased the moment carrying capacity, stiffness and reduce the deflection especially when the inner tube is square-shaped at the bottom. The curves follow an elastic path with decreasing stiffness until reaching the maximum bending capacity. However, the CFDSST specimens show greater stiffness and bending moment capacity than the control specimen. It can be seen that the control and CFDSST beams show ductile behavior. The control and CFDSST beams failed by rupture at the end of the test. For Group one showed that the maximum moment capacity for specimen S-S-50X50-B which have inner square tubes in the bottom as shown in Figure 4.11.

For group two showed that the maximum moment capacity for specimen S-S-40X40-B which have inner square tubes in the bottom, the specimens in this group have same deflection capacity as shown in Figures 4.12 and for group three showed that the specimens S-S-30X30-B which have inner square tubes in the bottom, as shown in Figures 4.13. In all groups the maximum moment capacity for the specimens have inner tube in bottom more than the specimens which have inner tubes in the center, but the moment capacity insignificant for the specimens have equivalent area and same inner tube position such as (square and rectangular) in center or (square and rectangular) in bottom.

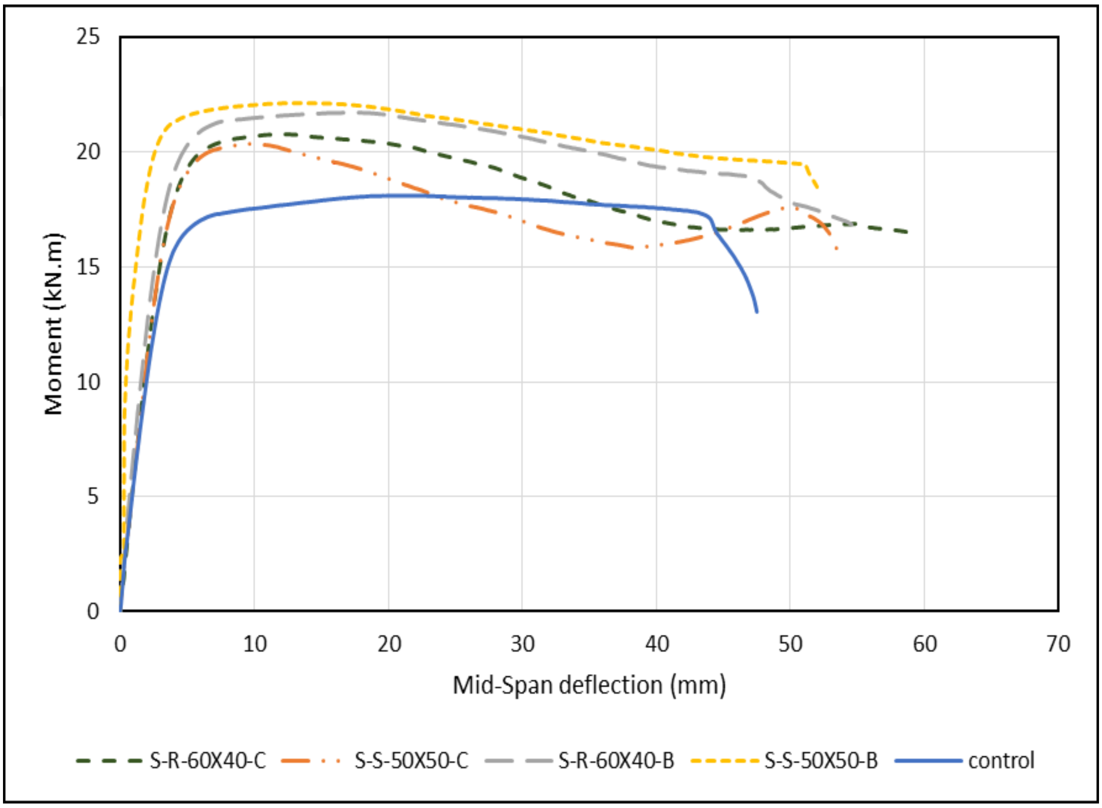

Figure 4.11 Moment capacity and mid span deflection for group one.

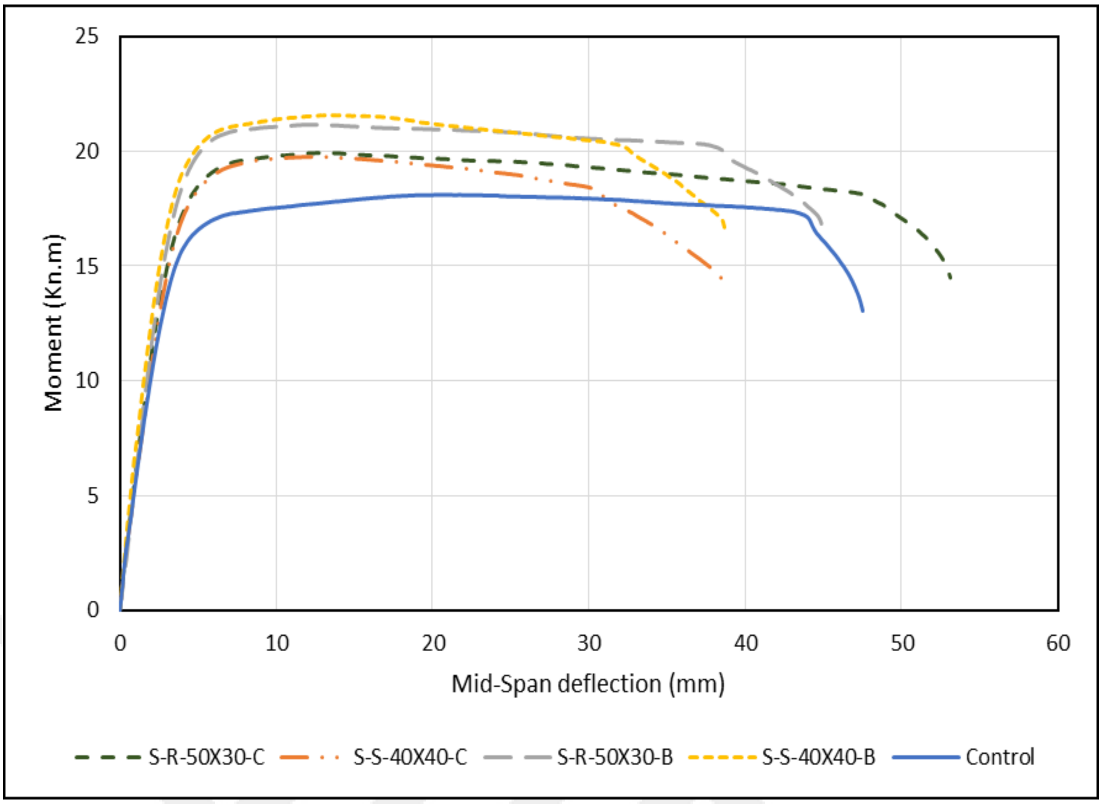

Figure 4.12 Moment capacity and mid span deflection for group two.

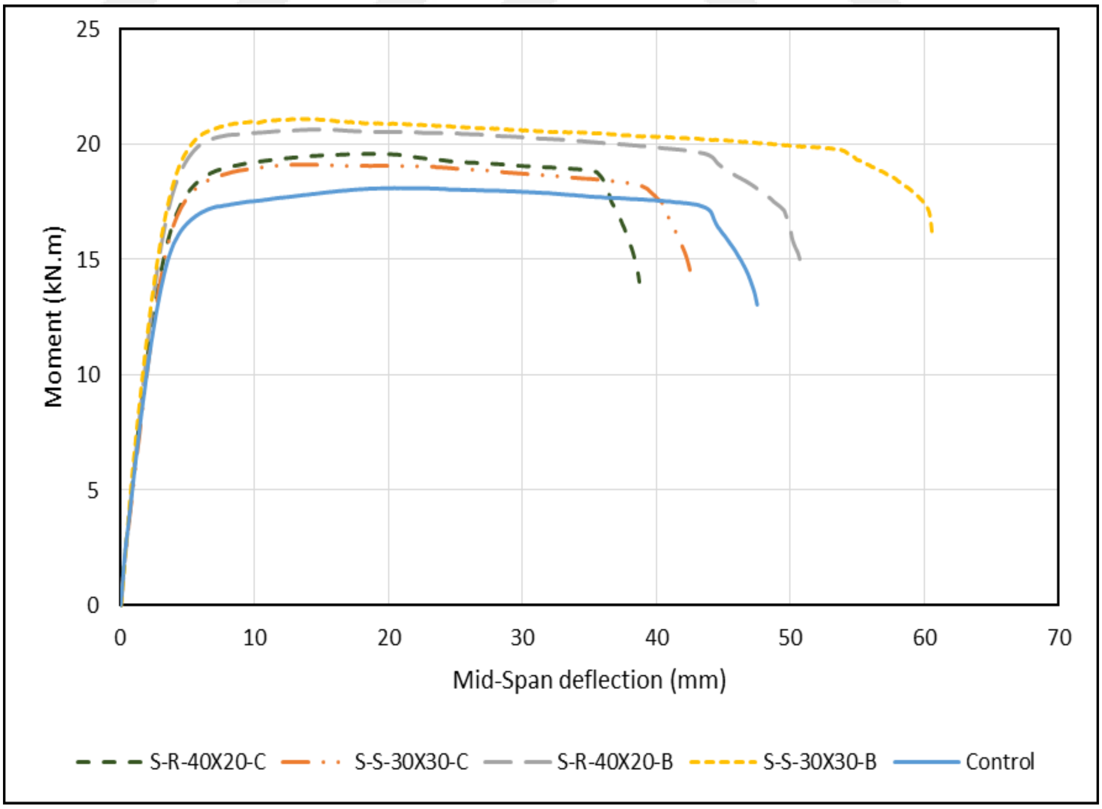

Figure 4.13 Moment capacity and mid span deflection for group three

4.4 Bending Moment Capacities

The maximum moments and percentage of increase in moment capacity for all groups specimens which have inner steel tube were compared them with the control beams without inner tube beam were summarized and tabulated.

Table 4.1 Moment and percentage of increase in moment capacity for group one.

Group name	Designation of beams	Moment (kN.m)	% increase in Moment.
	Control-beam	18.11	-----
Group one	S-R-60X40-C	20.77	14.69
	S-S-50X50-C	20.36	12.42
	S-R-60X40-B	21.73	19.99
	S-S-50X50-B	22.15	22.31

For group one the percentage are increase in the ultimate moment due to the inner steel tube from12.42% for specimen S-S-50X50-C to 22.31% for specimen S-S-50X50-B, also the specimens S-R-60X40-C and S-R-60X40-B have increase in moment 14.69% and 19.99% respectively. That means the advantage of changing the position of inner tube from center to bottom increase the moment capacity also use square shape in bottom better than use rectangular have equivalent area for square.

Table 4.2 Moment and percentage of increase in moment capacity for group two.

Group name	Designation of beams	Moment (kN.m)	% increase in Moment.
	Control-beam	18.11	-----
Group two	S-R-50X30-C	19.95	10.16
	S-S-40X40-C	19.78	9.22
	S-R-50X30-B	21.18	16.95
	S-S-40X40-B	21.60	19.27

The group two took the same behavior as the group one where it was percentage increase in the ultimate moment from 9.22% for specimen S-S40X40-C to 19.27% for specimen S-S40X40-B, also the specimens S-R50X30C and S-R50X30-B have increase in moment 10.16% and 16.95% respectively.

Table 4.3 Moment and percentage of increase in moment capacity for group three.

Group name	Designation of beams	Moment (KN.M)	% increase in Moment.
	Control-beam	18.11	-----
Group three	S-R-40X20-C	19.57	8.06
	S-S-30X30-C	19.15	5.74
	S-R-40X20-B	20.67	14.13
	S-S-30X30-B	21.11	16.57

The group three took the same behavior as the group one and two where it was percentage increase in the ultimate moment from 5.74% for specimen S-S-30X30-C to 16.57% for specimen S-S-30X30-B, also the specimens S-R40X20C and S-R-40X20-B have increase in moment 8.06 %and 14.13% respectively, also observed the group one have moment capacity more than group two and three which have same shape and position because the inner tube for group one have measurement larger than inner tube for group two and three. The Figure 4.13 shows the increase in moment capacity.

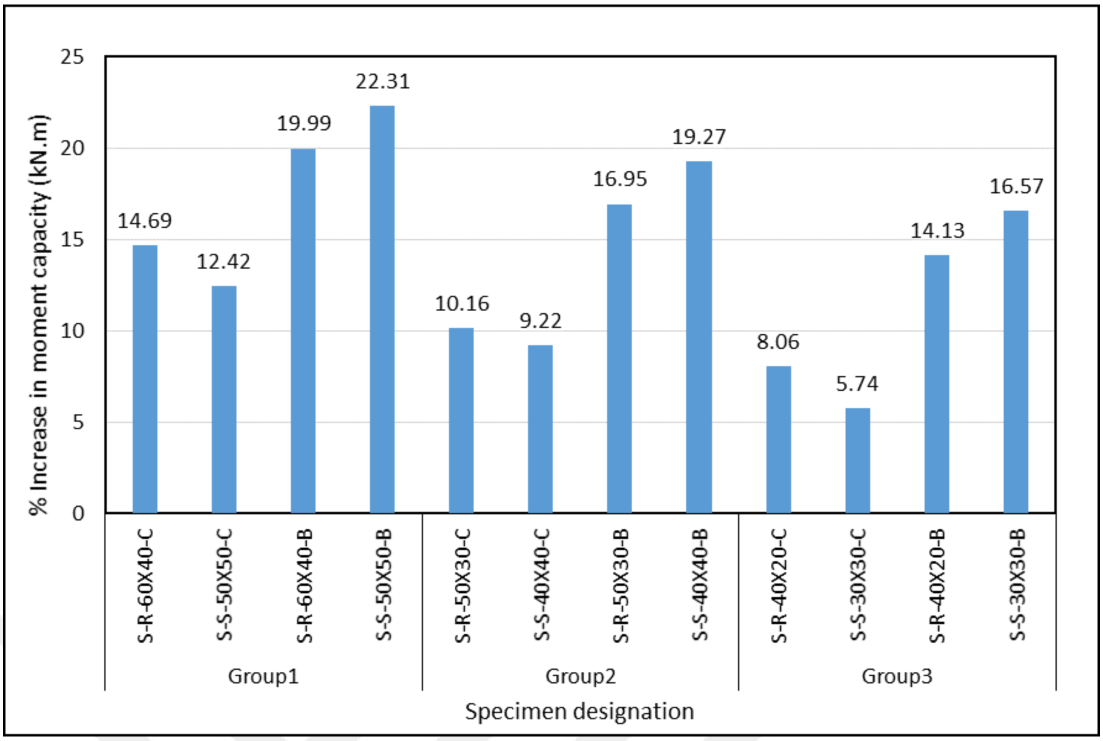

Figure 4.14 comparison in increase in moment capacity for all groups.

4.5 Ductility

Ductility is the ability of a material to undergo permanent deformation by elongation also, to withstand plastic deformation and bending without rupture. The ductility index (DI) of CFDSST had been determined for all groups as shown in Table 4.4-4.6.

Table 4.4 Deflection control and ductility index for group one.

Group name	Specimen	Mid span deflection Du. at Mu. (mm)	Mid span deflection Du. at (0.6Mu) (mm)	Ductility index Du / Du(0.6Mu)
	Control	20.15	2.56	7.87
Group one	S-R-60X40-C	12.25	2.35	5.21
	S-S-50X50-C	9.81	2.30	4.27
	S-R-60X40-B	17.47	2.15	8.13
	S-S-50X50-B	12.82	0.86	14.91

The ductility index ($DI=D_u/D_y$) which represents the ratio of mid-span deflection (D_u) at the ultimate moment (M_u) to the mid-span deflection (D_y) at $M = 0.6M_u$ was used to predict and compare the ductility of CFDSST beams compared to the control specimens. According to the obtained results for group one, the DI ranged from 4.27 for specimen S-S-50X50-C to 14.91 for specimen S-S-50X50-B. It is clear that the maximum DI obtained for the specimen S-S-50X50-B beams while for the control beam DI is 7.87. For specimen S-R-60X40-C and S-R-60X40-B DI is 5.21 and 8.13respectively.

Table 4.5 Deflection control and ductility index for group two

Group name	Specimen	Mid span deflection D_u at M_u (mm)	Mid span deflection D_u at (0.6Mu) (mm)	Ductility index D_u / D_u (0.6Mu)
	Control	20.15	2.56	7.87
Group two	S-R-50X30-C	13.20	2.20	6
	S-S-40X40-C	12.31	2.25	5.47
	S-R-50X30-B	12.41	2.10	5.91
	S-S-40X40-B	13.82	2.09	6.61

For group two, the DI ranged from 5.47 for specimen S-S-40X40C to 6.61 for specimen S-S-40X40B. The maximum DI for this group is 6.61 for specimen S-S-40X40-B. For specimen S-R50X30-C and S-R50X30-B DI is 6 and 5.91 respectively.

Table 4.6 Deflection control and ductility index for group three.

Group name	Specimen	Mid span deflection Du. at Mu. (mm)	Mid span deflection Du. at (0.6Mu) (mm)	Ductility index Du / Du(0.6Mu)
	Control	20.15	2.56	7.87
Group three	S-R-40X20-C	19.31	2.22	8.70
	S-S-30X30-C	13.15	2.25	5.84
	S-R-40X20-B	15.25	2.21	6.90
	S-S-30X30-B	13.25	2.17	6.11

For group three, the maximum DI is 8.70 for specimen S-R-40X20-C. The minimum Ductility Index DI is 5.84 for specimen S-S-30X30-C. For specimen S-R-40X20-B and S-S-30X30-B DI is 6.9 and 6.11 respectively. According to DI, the best value was obtained for a specimen S-S-50X50-B, also observe the square shape where it position in bottom (tension zone) give ductility greater than where it position in center. The Figure 4.15 explains ductility index for all groups.

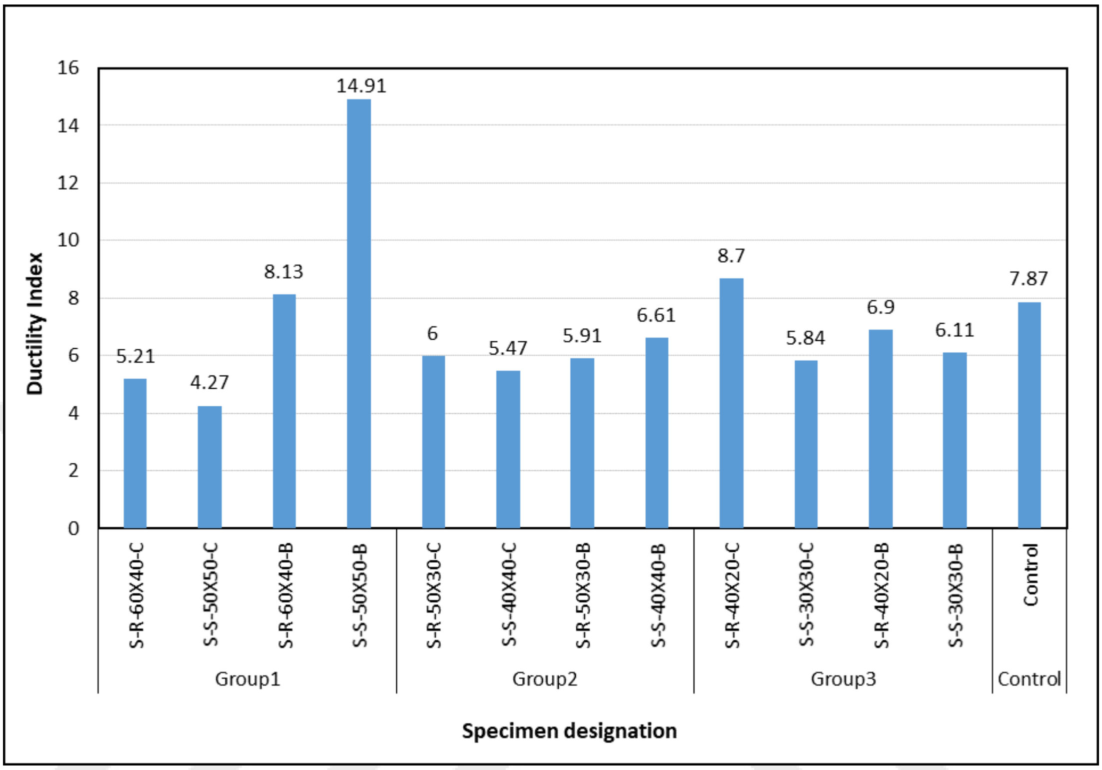

Figure 4.15 A comparison in ductility index among all specimens.

4.6 Flexural Stiffness Capacities

To assess and compare the flexural stiffness of the tested CFDSST two different stiffness values were used. The initial flexural strength corresponding to $M = 0.2M_u$, and the service- ability level flexural stiffness corresponding to $M = 0.6M_u$ in this study depended on (Han, L. 2004) and (Al-Shaar and GÖĞÜŞ 2018) to find the method of stiffness. Form results it was observed for the group one the highest value of the initial stiffness (K_i) was 928.04 kN.m for the specimen S-S-50X50-B and the lowest value was 314.83 kN.m for the specimen S-S-50X50C also it was observed that the highest value of flexural stiffness (K_s) was 905.34 kN.m for the specimen S-S-50X50-B and the lowest value was 302.99 kN.m. For the group two the highest value of the K_i was 418.98 kN.m for the specimen S-S-40X40-B and the lowest value was 322.54 kN.m for the specimen S-S-40X40C also it was observed that the highest value of K_s was

352.40 kN.m for the specimen S-S-40X40-B and the lowest value was 292.90 kN.m for the specimen S-S-40X40-C. For the group three the highest value of the initial K_i was 386.92kN.m for the specimen S-S-30X30-B and the lowest value was 342.60kN.m for the specimen S-S-30X30-C also it was observed that the highest value of K_s was 332.65kN.m for the specimen S-S-30X30-B and the lowest value was 291.10kN.m for the specimen S-S-30X30-C while the control gave Ks and Ki lower than all CFDSST specimens it was 312.57kN.m and 282.08kN.m respectively. From the result obtained that means Initial flexural stiffness and serviceability level flexural stiffness for CFDSST beams have square inner tubes in bottom better than other CFDSST beams also the K_s and Ki for all CFDSST better than the K_s and Ki for CFST beams. The table 4.7 explain Initial flexural stiffness and serviceability level flexural stiffness for CFDSST and control beams.

Table 4.7 Initial flexural stiffness and serviceability level flexural stiffness for CFDSST and control. m^2

Group name	Specimen	Ki (kN. m2)	Ks (kN. m2)
Group one	S-R-60X40-C	317.08	303.11
	S-S-50X50-C	314.83	302.99
	S-R-60X40-B	397.14	345.95
	S-S-50X50-B	928.04	905.34
Group two	S-R-50X30-C	338.63	306.67
	S-S-40X40-C	322.54	292.90
	S-R-50X30-B	343.39	319.38
	S-S-40X40-B	418.98	352.40
Group three	S-R-40X20-C	354.34	301.96
	S-S-30X30-C	342.60	291.10
	S-R-40X20-B	356.15	319.83
	S-S-30X30-B	386.92	332.65
Control	SC	312.57	282.08

4.7 Moment versus weight

In this study the weights were calculated for all specimens in groups. The lowest value of weight was in the group one was 26.42 (kg/m) and the highest moment capacity was 22.15 kN.m, while the control beam gave heights weight which 29.56 kg/m and lowest moment capacity was 18.11kN.m. That's means one of advantages of CFDSST give high moment capacity with little weight. The Table 4.8 explain moment capacity and weight for specimens.

Table 4.8 Moment capacity and weight for specimens.

Group name	Specimen	Moment capacity (kN.m)	% increase in Moment.	Weight of beam (kg/m)
Group one	S-R-60X40-C	20.77	14.69	26.42
	S-S-50X50-C	20.36	12.42	26.42
	S-R-60X40-B	21.73	19.99	26.42
	S-S-50X50-B	22.15	22.31	26.42
Group two	S-R-50X30-C	19.95	10.16	28.05
	S-S-40X40-C	19.78	9.22	28.05
	S-R-50X30-B	21.18	16.95	28.05
	S-S-40X40-B	21.60	19.27	28.05
Group three	S-R-40X20-C	19.57	8.06	29.17
	S-S-30X30-C	19.15	5.74	29.17
	S-R-40X20-B	20.67	14.13	29.17
	S-S-30X30-C	21.11	16.57	29.17
Control	SC	18.11	-------	29.56

CHAPTER 5

CONCLUSIONS AND RECOMMENDATIONS

5.1 Conclusions

In this study, the results of an experimental study to investigate of flexural performance of CFDSST beams. Based on the experimental result, the following conclusion can be indicated

- The inner tube enhances the strength capacity of CFDSST, when change the shape of inner tube from rectangle to square there is little difference between them in the strength capacity but when change the position of inner tube from center to bottom observe obvious effect on the strength capacity, where the position of the inner tube at the bottom (tension zone) gives more strength when it position in the center.

- Failure modes: The specimens of CFDSST outward buckling occur for outer tube and inward buckling occur for inner tube, two specimens outward buckling occur in two points (all the specimens of CFDSST give a failure mode as a filled tube for outer tube and give failure mode as a hollow tube for inner tube) For all the specimens rupture occur in end of test.

- The deflection curves along effective length with different moment levels followed approximately the half sine wave curve during the course of the entire test.

- The initial flexural strength and serviceability level flexural stiffness for specimens have inner tube in the bottom better than for the specimens have inner tube in the center, especially for the square shape in all groups.

- According to the result, the ductility index for specimens have inner tube in the bottom better than for the specimens have inner tube in the center, especially for the square shape.

- The highest ultimate moment capacity in CFDSST beams is about 22.31% for group one, 19.27% for group two, and 16.57% for group three as compared to their control beams.

- The highest maximum moment capacity due to inner tube in CFDSST beams as compared to the other is about 22.15 kN.m for group one, 21.60 kN.m for group two, and 21.11 kN.m for group three.

- The lowest moment capacity for CFDST beams as compared to the other is about 20.36 for group one, 19.78 kN.m for group two, and 19.15 kN.m for group three. In all groups CFDSST give moment capacity larger than control beam.

- The minimum weight for group one is about 26.42kg/m the maximum weight for control beam was 29.56kg/m

- From the results in this research the tube S-S-50X50B which have inner tube in bottom and square shape give high stiffness, high moment strength, high ductility and light weight that mean use this shape and position for specimen in structural construction better than other specimens.

5.2 Recommendations

Few of previous studies were conducted on the position of inner tube for the CFDSST beams. According to the test results in this study, it was found that using of inner tube in the bottom (tension zone) led to increase the moment capacity, flexural stiffness, and ductility. In the future many researches can be conduct on this kind of beams by using another dimensions and another shapes of outer and inner tubes. Also, finite element method can be utilize on this kind of beam and comparing the results with the experimental results.

REFERENCES

Alfawakhiri, F. (1997). Behavior of High-Strength Concrete-Filled Circular Steel Tube Beam-Columns, *University of Ottawa* ***(Canada)***.

Al-Shaar, A. A.,Göğüş, M. T. (2018). Flexural Behavior of Lightweight Concrete and Self-Compacting Concrete-Filled Steel Tube Beams. *Journal of Constructional Steel Research*, **149**, 153-164.

BIBM, C., ERMCO, E. e EFNARC, "The European Guidelines for Self-Compacting Concrete," (2005).

Chapman., J,C. (1964). Experiments on Composite Beams, *Journal of Structural Engineering*, **42**, 369–383.

Chen, J., Ni, Y. Y.,Jin, W. L. (2015). Column Tests of Dodecagonal Section Double Skin Concrete-Filled Steel Tubes. *Thin-Walled Structures*, **88**, 28-40.

Chen, J., Wang, J., Xie, F., Jin, W. L. (2016). Behavior of Thin-Walled Dodecagonal Section Double Skin Concrete-Filled Steel Tubes under Bending. *Thin-Walled Structures*, **98**, 293-300.

Chitawadagi, M. V., Narasimhan, M. C. (2009). Strength Deformation Behaviour of Circular Concrete Filled Steel Tubes Subjected to Pure Bending, *Journal of constructional steel research*, **65(8)**, 1836-1845.

Elchalakani, M., Zhao, X. L., Grzebieta, R. (2002). Tests on Concrete Filled Double-Skin (CHS outer and SHS inner) Composite Short Columns under Axial Compression. *Thin-walled structures*, **40(5)**, 415-441.

Elchalakani, M., Zhao, X. L., Grzebieta, R. H. (2001). Concrete-filled circular steel Tubes Subjected to Pure Bending, *Journal of Constructional Steel Research*, **57(11)**, 1141-1168.

Ghannam, S. (2016). Flexural Strength of Concrete-Filled Steel Tubular Beam with Partial Replacement of Coarse Aggregate by Granite, *International Journal of Civil Engineering and Technology **(IJCIET)***, **7**, 161-168.

Han, L. H. (2004). Flexural Behaviour of Concrete-Filled Steel Tubes, *Journal of Constructional Steel Research*, **60(2)**, 313-337.

Han, L. H., Huang, H., Zhao, X. L. (2009). Analytical Behaviour of Concrete-Filled Double Skin Steel Tubular (CFDST) Beam-Columns Under Cyclic Loading. *Thin-walled structures,* **47(6-7)**, 668-680.

Han, L. H., Huang, H., Tao, Z., Zhao, X. L. (2006). Concrete-Filled Double Skin Steel Tubular (CFDST) Beam–Columns Subjected to Cyclic Bending. *Engineering Structures*, ***28*(12)**, 1698-1714.

Han, L. H., Li, W., Bjorhovde, R. (2014). Developments and Advanced Applications of Concrete-Filled Steel Tubular (CFST) Structures: Members, *Journal of Constructional Steel Research*, **100**, 211-228.

Han, L. H., Tao, Z., Huang, H., Zhao, X. L. (2004). Concrete-filled double skin (SHS outer and CHS inner) steel tubular beam-columns. *Thin-walled structures*, **42(9),** 1329-1355.

Hou, C., Han, L. H., Zhao, X. L. (2015). Behaviour of Circular Concrete Filled Double Skin Tubes Subjected to Local Bearing Force. *Thin-Walled Structures*, **93**, 36-53.

Hu, H. T., Huang, C. S., Wu, M. H., Wu, Y. M. (2003). Nonlinear Analysis of Axially Loaded Concrete-Filled Tube Columns with Confinement Effect. *Journal of Structural Engineering*, ***129*(10)**, 1322-1329.

Idris, Y., & Ozbakkaloglu, T. (2015). Flexural Behavior of FRP-HSC-Steel Double Skin Tubular Beams under Reversed-Cyclic Loading. *Thin-Walled Structures*, **87**, 89-101.

Issam Assi, Serein M, Abed and Yasser M Hunaiti (2002). Flexural Strength of Composite Beams Partially Encased in Lightweight Concrete, *Pakistan journal of applied science* ***2*(3),** 320-323.

L. Yam, C. P., and C. J. C., (1968). The Inelastic Behavior of Simply Supported Composite Beams of Steel and Concrete, *Proceedings of the institution of civil engineers,* **41.4**, 661–683.

Li, W., Han, L. H., Chan, T. M. (2014). Tensile Behaviour of Concrete-Filled Double-Skin Steel Tubular Members. *Journal of Constructional Steel Research*, **99***,* 35-46.

Li, W., Han, L. H., Chan, T. M. (2015). Performance of Concrete-Filled Steel Tubes Subjected to Eccentric Tension, *Journal of Structural Engineering*, **141(12)**.

Lin-Hai Han, Hui Lu, Guo-Huan Yao and Fei-Yu Liao (2006). Further Study on the Flexural Behaviour of Concrete-Filled Steel Tubes, *Journal of Constructional Steel Research, **62***, (2006) 554–565.

M. Lachemi , K.M.A Hossain and V.B. Lambors (2006). Self-consolidating concrete filled steel tube column– Design equations for confinement and axial strengths, *structural engineering and mechanics,* **22(5)**, 541-562.

Montague, P. (1978). The Experimental Behaviour of Double-Skinned, Composite, Circular Cylindrical Shells under External Pressure. *Journal of Mechanical Engineering Science*, **20(1)**, 21-34.

Oduyemi, T. O. S., Wright, H. D. (1989). An experimental investigation into the behaviour of double-skin sandwich beams. *Journal of Constructional Steel Research,* **14(3)**, 197-220.

Roberts, T., and M., (1985). Finite Difference Analysis of Composite Beams with Partial Interaction, *Journal Computers & structures.* **21**, 469–473.

Tao, Z., Han, L. H. (2006). Behaviour of concrete-filled double skin rectangular steel tubular beam–columns. *Journal of Constructional Steel Research,* **62(7),** 631-646.

Tao, Z., Han, L. H., Zhao, X. L. (2004). Behaviour of Concrete-Filled Double Skin (CHS inner and CHS outer) Steel Tubular Stub Columns and Beam-Columns. *Journal of Constructional Steel Research,* **60(8)**, 1129-1158.

Uenaka, K. (2013). Concrete Filled Double Skin Circular Tubular Beams with Large Diameter-to-Thickness Ratio under Shear. *Thin-Walled Structures,* **70**, 33-38.

Uenaka, K., Kitoh, H. (2011). Mechanical Behavior of Concrete Filled Double Skin Tubular Circular Deep Beams. *Thin-Walled Structures*, **49(2)**, 256-263.

Varma, A. H., Ricles, J. M., Sause, R., Lu, L. W. (2002). Seismic Behavior and Modeling of High-Strength Composite Concrete-Filled Steel Tube (CFT) Beam–Columns, *Journal of Constructional Steel Research*, **58(5)**, 725-758.

Venkatesh, A., Sivakamasundari, S. (2017). Experimental Study of Concrete Filled Double Skin Tubular Structures in Bending. *International Journal of Civil Engineering and Technology,* **8(4).**

Wang, F., Young, B., Gardner, L. (2017, November). Structural Performance of Concrete-Filled Double Skin Tubular Beams with Eccentric Inner Tubes. In Tubular Structures XVI: *Proceedings of the 16th International Symposium for Tubular Structures (ISTS 2017, 4-6 December 2017, Melbourne, Australia)* **(p. 117).** CRC Press.

Yam, L.C.P., and Chapman J.C., (1972). The Inelastic Behaviour of Continuous Composite Beams of Steel and Concrete, *Institution of Civil Engrs, Pt2, Research & Theory 53. Proceeding,* **53**, 487–501.

Yang, Y. F., Hou, C., Meng, C. Y., Han, L. H. (2015). Investigation on Square Concrete Filled Double-Skin Steel Tube (CFDST) Subjected to Local Bearing Force: Experiments. *Thin-Walled Structures*, **94**, 394-409.

Zhao, XL, and Grzebieta, R.H., (1999), "Void-Filled SHS Beams Subjected to Large Deformation Cyclic Bending", *Journal of Structural Engineering*, **Vol 128**, No 9, pp 1020-1027.

Zhao, X. L., Han, L. H. (2006). Double Skin Composite Construction. *Progress in structural engineering and materials*, **8(3)**, 93-102.

Zhao, X. L., Han, B., Grzebieta, R. H. (2002). Plastic Mechanism Analysis of Concrete-Filled Double-Skin (SHS inner and SHS outer) Stub Columns.*Thin-Walled Structures*, **40(10)**, 815-833.

Zhou, M., Xu, L.Y., Tao, M.X., Fan, J. S., Hajjar, J. F., Nie, J. G. (2017).Experimental Study on Confining-Strengthening, Confining-Stiffening, and Fractal Cracking of Circular Concrete Filled Steel Tubes Under Axial Tension, *Engineering Structures*, **133**, 186-199.